IEEE Access
Multidisciplinary | Rapid Review | Open Access Journal

Received March 8, 2022, accepted March 16, 2022, date of publication March 22, 2022, date of current version March 30, 2022.

Digital Object Identifier 10.1109/ACCESS.2022.3161505

Adaptive LFC Incorporating Modified Virtual Rotor to Regulate Frequency and Tie-Line Power Flow in Multi-Area Microgrids

HUSSEIN ABUBAKR[1,2], (Graduate Student Member, IEEE), JOSEP M. GUERRERO[1], (Fellow, IEEE), JUAN C. VASQUEZ[1], (Senior Member, IEEE), TAREK HASSAN MOHAMED[2], KARAR MAHMOUD[3,4], (Senior Member, IEEE), MOHAMED M. F. DARWISH[3,5], (Member, IEEE), AND YASSER AHMED DAHAB[6]

[1]Center for Research on Microgrids (CROM), AAU Energy, Aalborg University, 9220 Aalborg, Denmark
[2]Department of Electrical Engineering, Faculty of Energy Engineering, Aswan University, Aswan 81528, Egypt
[3]Department of Electrical Engineering and Automation, School of Electrical Engineering, Aalto University, 02150 Espoo, Finland
[4]Department of Electrical Engineering, Faculty of Engineering, Aswan University, Aswan 81542, Egypt
[5]Department of Electrical Engineering, Faculty of Engineering at Shoubra, Benha University, Cairo 11629, Egypt
[6]College of Computing and Information Technology, Arab Academy for Science, Technology and Maritime Transport, South Valley Branch, Aswan 81516, Egypt

Corresponding authors: Hussein Abubakr (haha@energy.aau.dk) and Karar Mahmoud (karar.mostafa@aalto.fi)

The work of Hussein Abubakr was fully funded by the Ministry of Higher Education of the Arab Republic of Egypt; and supported by VILLUM FONDEN under the VILLUM Investigator through the Center for Research on Microgrids (CROM) under Grant 25920.

ABSTRACT This research investigates a new coordination strategy for both isolated single-area and interconnected multi-area microgrids (MGs) using a modified virtual rotor-based derivative technique supported with Jaya optimizer based on balloon effect modulation (BE). Accordingly, the main concept of BE is to assist the classic Jaya to be more sensitive and trackable in the event of disturbances, as well as to provide optimum integral gain value on the secondary frequency controller adaptively for both suggested MGs. The proposed modified virtual rotor mechanism is consisting of virtual inertia and virtual damping that are added as a tertiary controller within proposed MGs considering full participation of the inverter-based energy storage systems. The proposed virtual rotor mechanism is consisting of virtual inertia and virtual damping that are added as a tertiary controller within proposed MGs to emulate the reduction in system inertia and the enhanced damping properties. Several nonlinearities were proposed in this work such as a dead band of governor, generation rate constraints, and communication time-delay are considered within the dynamic model of the suggested MGs. In addition, the proposed design of multi-area MGs takes the interval time-varying communication delays into account for stability conditions. In this study, A comparative study using unimodal (i.e., Sphere) and multimodal (i.e., Rastrigin) benchmark test functions are conducted to validate the proposed direct adaptive Jaya-based BE. Furthermore, Wilcoxon's rank-signed non-parametric statistical test using a pairwise comparison was performed at a 5 % risk level to judge whether the proposed algorithm output varies from those of the other algorithms in a statistically significant manner. Thence, the superiority and effectiveness of the proposed method have also been verified against a variety of other metaheuristics optimization techniques, including classic electro-search, particle swarm, multi-objective seagull, and Jaya optimizers. In addition, an operative performance is assessed against the conventional integral controller, coefficient diagram method, and classic Jaya with/without virtual inertia. The final findings emphasize the superiority of the proposed direct adaptive Jaya-based BE supported by a modified virtual rotor and state better performance and stability compared to existing controllers.

INDEX TERMS Multi-area microgrids, virtual damping, virtual inertia, Jaya technique, adaptive control, balloon effect, coefficient diagram method, frequency regulation, time-varying delay.

NOMENCLATURE

Δf	Frequency deviation (Hz).
ΔP_g	Governor output power change.
ΔP_d	Diesel power change.
ΔP_c	Change in speed changer position.
ΔP_L	Change in electrical demand load.
ΔP_{WT}	Change in wind power.
$\Delta P_{Tieline}$	Tile-line power change.

The associate editor coordinating the review of this manuscript and approving it for publication was Wei Liu.

$\Delta P_{Inertia}$	Change in virtual rotor power.
β_i	Tie-line frequency bias of area (i) (pu/Hz).
D_o	Equivalent damping coefficient (pu/Hz).
M_o	Equivalent inertia constant (pu.sec).
R	Speed droop characteristic (Hz/pu).
$T_{i,j}$	Synchronizing coefficient of tie-line with an area- j.
T_{ESS}	Inverter-based ESS time constant (sec).
T_d	Diesel time constant (sec).
T_g	Governor time constant (sec).
T_r	Rise time (sec).
T_s	Settling time (sec).
M_P	Maximum overshoot.
ω_n	Natural frequency.
η	Damping ratio.
AL	Acceleration coefficient parameter for BE.
$J_{VI,i}$	Virtual inertia coefficient.
$D_{VI,i}$	Virtual damping coefficient.
α_o	Participation ratio coefficient.
R^+	Sum of the positive difference ranks.
R^-	Sum of the negative difference ranks.
d_i	Continuous difference.
α	Risk level (level of significance).
p	Probability value.
y	The system output.
τ	Equivalent time constant.
γ_i	Stability indices.
γ_i*	Stability limits.
r	Reference input.
d	External disturbance input.
u	Actuating signal for the closed-loop.
$N(s)$	Numerator of the plant transfer function.
$D(s)$	Denominator of the plant transfer function.
$F(s)$	Input numerator polynomial of the controller transfer function.
$A(s)$	Denominator polynomial of the controller transfer function.
$B(s)$	Feedback numerator polynomial of the controller transfer function.
$P(s)$	Characteristic polynomial of the closed-loop system.
K_i	Coefficients of the controller polynomial.
L_i	Coefficients of the controller polynomial.
a_i	Coefficients of the characteristic polynomial P(s).
h	Maximum upper bound delay.
$d(t)$	Delay communication time in (sec).
μ	Varying coefficient for initial time.
MG	Microgrid system.
BE	Balloon Effect.
ESS	Energy storage system.
ACE	Area control error.
GRC	Generation rate constraints.
CDM	Coefficient diagram method.
ESO	Electro-search optimization technique
PSO	Particle swarm optimization technique.
ANOVA	Analysis of variance.

I. INTRODUCTION

Generally, microgrids (MGs) have two types of operation: grid-connected and islanded operation modes [1], [2]. For islanded patterns, systems for storage and traditional diesel generators are typically responsible for frequency regulation. While a connected mode for the grid, the bulk power system handles the frequencies [3], [4]. The variability of renewable energy sources (RESs) power generations leads to high perturbations in power flow and frequency in the MG, and this will greatly affect the MG operation. Therefore, the high penetration of RESs makes the situation in MG worse due to low inertia and damping; Thus, it creates some issues in stabilizing system frequency and voltage, resulting in a weakening of the MG stability and flexibility. For this point, integrated resource planning in sustainable energy-based distributed microgrids has been alleviated in [5] to solve the issue of intermittency of RESs and to assess the optimal allocation of these suitable integrated resources planning for eco-friendly sustainable energy-based hybrid microgrids with distributed generation.

A. LITERATURE REVIEW

In recent years, distributed generation has had an increasing impact on distribution grids [6]. As the number of active users is increasing in grid dynamics, but due to the presence of certain technical and standards issues, they don't participate in the grid administration. To strengthen the service cohesion, generators and active users ought to be involved in a grid management coordination procedure [7]–[9]; Given this approach to islanded operation, it could be a major key to shifting from traditional into smart grids.

Low system inertia occurs because of the connection of the inverter/converter with RESs to MGs. These devices don't have any damping or inertia properties that may lead to significant frequency deviations and system instability as mentioned in [10]. To mitigate the lack of inertia and weak anti-disturbance capability of frequency in MGs, a lot of inertia control techniques have been used to resolve MG frequency control issues, thereby enhancing the stability of frequency [10]–[18]. An adaptive virtual inertia-damping system has been suggested in [11] using the concept of model predictive control (MPC), which relies on the frequency performance enhancement of islanded MGs taking into account the high RESs penetration level. Recently, modified virtual inertia and damping based on derivative control techniques have been utilized to support the stability of frequency in small and large grids [12], [13]. The concept of virtual inertia has been proposed to support the stability of frequency in AC/DC interconnected grids [14], and the

virtual inertia is suggested with phase-locked loop impact on deregulated automatic generation control system integrated with parallel AC/HVDC and a novel methodology for tapping of RES potential using virtual inertia are discussed in [15], [16]. In [17], a virtual inertia control based on fuzzy logic- MPC systems have been applied to regulate the frequency. A hierarchical and adaptive control schemes for frequency and voltage regulation in multi-area microgrid considering virtual synchronous generators are presented in [18], [19].

Getting a proper match between nominal and robust performance is difficult when using old and conventional approaches. Moreover, uncertainty combinations (i.e., modeling of unstructured uncertainty) for control techniques haven't been considered and designed. So, it is difficult to attain both performance and stability in a wide range of uncertainties and disturbances using the abovementioned methods of controlling. Because of the possibility of formulating uncertainty in the control structure procedure, powerful control approaches can effectively solve this issue, such as the MPC used in [20], [21], to deal with the interrelationship between control loops of frequency and voltage excitation, resulting in poor performance of the system. Several works have been made for measuring and evaluating the performance of AGC different power systems applications considering renewable energy sources such as in [22], [23]. Another powerful controller called the coefficient diagram method (CDM) was depicted in [24]. Basically, the CDM is an algebraic method that is applied to a polynomial loop in the parameter space, this controller is proposed in this work for comparison with the proposed direct adaptive Jaya-based BE supported by a modified virtual rotor.

Time delays have appeared frequently in many modern industrial control processes in practice to study their impact in power system applications and are further discussed in [25], [26]. Also, time delay leads to oscillation or instability of the control system in many cases. Therefore, a study on the stability of the dynamical model is attracted by many researchers [27], [28]. The major goal in the study of stability analysis for the control system with time delay is to expand the region of the feasibility for maximizing the upper delay bounds of the discussed control system, which also guarantees the system's stable performance with given constraints.

Frequency regulation is a critical issue in MGs to sustain the changes in power and system frequency at their set points. To cope with the instability issue, several attempts made to implement optimization techniques [29]–[40] have been used to adjust the controller parameters in the context of adaptive control issue based on soft computing techniques, to solve the complexity in construction and two-adaptive shape as presented in [41], [42] which applied indirectly, and this takes more time for computation that is considered very important in control interval law.

On the other hand, the multi-objective seagull has proposed in [40] built on the concept of the dynamic archive which has the feature to cache the non-dominated Pareto optimal solutions. In addition, another mathematical optimizer called Jaya has been proposed in [43] due to it has many benefits such as parameters tuning is not needed at the computations time and can resolve both unrestricted and constrained issues, and is appropriate for discrete optimization problems. In addition, the controller parameters of the algorithm for every moment can be easily determined in less time.

Literature has shown that some algorithms have good/bad performance in the implementation of some widely used benchmark functions. The statistical analysis using best, worst, and mean values is not sufficient to verify the effectiveness of optimizers against others. Therefore, we suggested in this research using a non-parametric statistical analysis as introduced before in [44] to validate the proposed Jaya-based BE against other algorithms considering ANOVA test, and also supported with the speed convergence test using unimodal and multimodal benchmark functions.

B. MOTIVATIONS AND LIMITATIONS

As mentioned in the literature, the variability of RESs and random loads lead to more oscillations in power flow and frequency in the MGs and to poorer response to the common point of coupling (PCC) and active and reactive powers transfer. this penetration resulting from RESs causes some difficulties in regulating the frequency and voltage, resulting in a weakening of the MG stability and resiliency. As a result, severe deviations in system frequency hurt the control performance parameters, and this will cause energizing of under/over frequency relay and disconnect some loads. The conventional controller such as I, PI, and PID can't resolve the uncertainties situation. Also, there are several robust controllers as mentioned in the literature rely on the controller design such as MPC, H∞, CDM, fuzzy logic, and two-step adaptive concept-based optimizers have some design drawbacks and it takes a long time to define the control parameters, and this is not appropriate for control interval.

Based on the above observations, this work investigates a coordination scheme between LFC and modified virtual rotor interaction that aims to modify the stability and performance of MG frequency and power regulation in tie-line, using the direct adaptive concept of Jaya-based balloon effect (BE) considering the virtual rotor and virtual damping. The modulation of BE was added to the classic Jaya to raise the algorithm sensitivity to load perturbations and changes in system parameters. In addition, BE has also used the open-loop plant inputs and outputs to determine the actual on-time transfer function including disturbances and variations in parameters for the plant.

C. CONTRIBUTION AND PAPER ORGANIZATION

The main reason to write this manuscript is as follows:

i. The concept of direct adaptive Jaya-based balloon effect modulation supported by a modified virtual rotor considering full participation of the inverter-based ESS has been demonstrated.

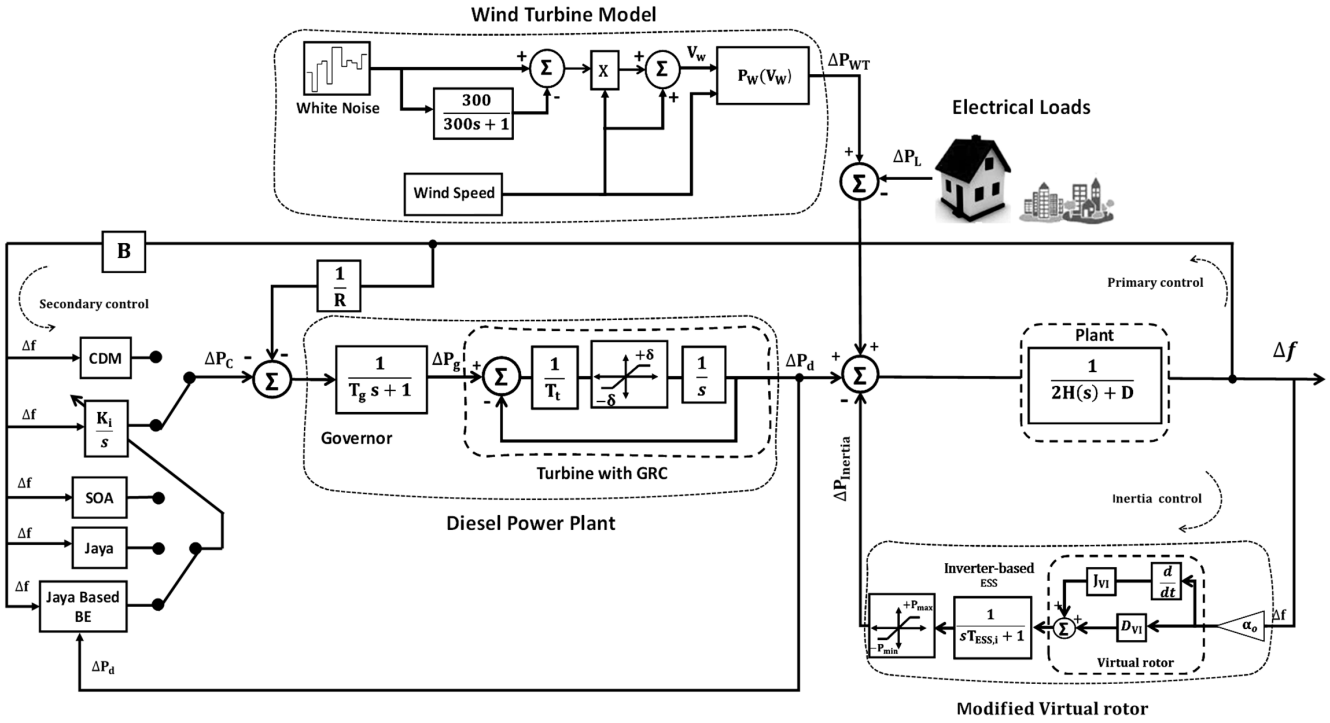

FIGURE 1. A dynamic model of the studied islanded MG with the proposed modified virtual rotor.

ii. The concept of BE modulation is compiled to the classic Jaya optimizer to increase the algorithm interactivity and sensitivity with the online system issues.
iii. A non-parametric statistical analysis and ANOVA test have been carried out to validate the performance superiority of the proposed Jaya-based BE.
iv. System nonlinearities such as GDB, GRCs, time-varying communication delay are considered within the dynamic MG model.
v. The proposed control strategy is compared with I/CDM-based LFC with/without the participation of virtual inertia under the effect of partial/full injection of wind energy and random load variations for both MGs.

The rest of this manuscript is outlined as follows: Section II describes the proposed islanded single area MG dynamic model. Section III illustrates the main control strategy of the modified virtual rotor mechanism. The coefficient diagram method as a robust controller is presented in section IV. A general overview of the classic Jaya and multi-objective seagull optimizers are presented in section V. The main concept of the balloon effect is introduced in section VI. Jaya-based adaptive frequency control with/without the balloon effect is presented in section VII. The performance analysis of the proposed Jaya-based BE is framed in section VIII. Section IX demonstrates the final findings and provides a discussion on the suggested controlled system. Section X introduces multi-are MGs application supported with time-varying delay. The final findings are concluded and offered in section XI.

II. MICROGRID MODELLING

A. SINGLE AREA ISLANDED MICROGRID

This paper focuses on an islanded MG (20 MW base), which consists of a non-reheated turbine power plant with a capacity of 20 MW, 17 MW of electrical loads, and 6 MW from wind farm (details in Appendix). The RESs power variance, as wind fluctuation and load variation, were considered signs of turbulence for the suggested MG. Figure 1 describes the block diagram of the studied single area MG dynamic model.

The following equations can depict the suggested single-area MG dynamic model. The total load-generator dynamic relationship between the supply error and frequency distortion can be expressed as:

$$\Delta f = \left(\frac{1}{2Hs + D}\right)(\Delta P_M - \Delta P_L) \tag{1}$$

where,

$$\Delta P_M = (\Delta P_d \pm \Delta P_{Inertia} + \Delta P_{wind}) \tag{2}$$

$$\Delta P_d = \left(\frac{1}{T_t s + 1}\right)\Delta P_g \tag{3}$$

$$\Delta P_g = \left(\frac{1}{T_g s + 1}\right)\left(\Delta P_c - \frac{1}{R}\Delta f\right) \tag{4}$$

$$\Delta P_{Inertia} = \alpha_o \left(\frac{J_{VI} s + D_{VI}}{1 + sT_{ESS}}\right)[(\Delta f)] \tag{5}$$

$$\Delta P_{WT} = \left(\frac{1}{T_{WT} s + 1}\right)\Delta P_{Wind} \tag{6}$$

The dynamic equations of the studied MG in state variable form can be written and derived as follows:

$$\dot{X} = AX + BU + EW \tag{7}$$
$$Y = CX + DU + FW \tag{8}$$

(9) and (10), as shown at the bottom of the page, where,

$$X^T = [\Delta f\, \Delta P_g \Delta P_d \Delta P_{WT} \Delta P_{Inertia}]$$
$$W^T = [\Delta P_{wind}\, \Delta P_L]$$
$$Y = [\Delta f]$$

where $\Delta P_d, \Delta P_L, \Delta P_{Inertia}, \Delta P_g, \Delta P_{wind}$ *and* ΔP_c are changes in diesel, load, inertia, governor, wind, and supplementary control power respectively. D is the damping coefficient, R is the governor speed regulation, H is the overall system inertia, and D is the damping coefficient. T_{ESS} is the inverter-based energy storage system (ESS) time constant that is used to emulate the ESS dynamic control in the isolated and interconnected MGs. α_o, J_{VI}, and D_{VI} mean the participation ratio coefficient, the virtual inertia, and damping constants. The criteria for choosing the virtual inertia and damping coefficients are concerning the desired dynamic response and MG stability. Here in this study, the virtual parameters are obtained using the Eigenvalue analysis as discussed in [13].

III. MODIFIED VIRTUAL ROTOR CONTROL

In islanded and interconnected MGs, several control issues may occur due to the non-uniform RESs nature such as frequency instability issues, which may boundary their penetration. As a result, MGs are becoming more susceptible to disturbances than traditional ones, and thus encounter disturbances such as abrupt disconnection in loads and short-circuit faults with long clearance times [45], [46]. Therefore, the concept of the modified virtual rotor (inertia + damping) considering full participation of inverter-based ESS ($\alpha_o = 100\%$) can be used to compensate for the inertia induced by RESs in the isolated and interconnected MGs and enhance the low-damping properties. In this work, an ESS has been applied as a source of a virtual inertia power used to emulate the kinetic energy as found in a real synchronous generator.

The law of the control strategy using ESS based derivative technique is shown in Fig. 2. The strategy is to add sufficient active power to the community by calculating the ROCOF using a derivative technique [10], [13]. Therefore, the suggested modified virtual inertia structure can diminish the desired power system inertia and damping characteristics, resulting in the enhancement of the overall inertia within the MG system, frequency stability, and preventing outage of the power. The power provided by the modified virtual rotor control system to the MG is described in Eq. (5).

IV. COEFFICIENT DIAGRAM METHOD

CDM can be classified as an algebraic design algorithm in which the bode diagram has been replaced by coefficient one. CDM is considered a method of arranging the closed-loop poles to reach the desired system time response [47].

Figure 3. illustrates the block diagram of the CDM algorithm for a single-input-single-output (SISO) linear time-invariant system.

The system's output can be described as:

$$y = \frac{N(s)F(s)}{P(s)}r + \frac{A(s)N(s)}{P(s)}d \tag{11}$$

$$\dot{X} = \begin{vmatrix} \frac{-D}{2H} & 0 & \frac{1}{2H} & \frac{1}{2H} & \frac{1}{2H} & \frac{1}{2H} \\ \frac{-1}{RT_g} & \frac{-1}{T_g} & 0 & 0 & 0 & 0 \\ 0 & \frac{1}{T_t} & \frac{-1}{T_t} & 0 & 0 & 0 \\ 0 & 0 & 0 & \frac{-1}{T_{wind}} & 0 & 0 \\ \frac{(J_{VI}+D_{VI})*D}{T_{Ess}*2H} & 0 & \frac{(J_{VI}+D_{VI})}{T_{Ess}*2H} & \frac{(J_{VI}+D_{VI})}{T_{Ess}*2H} & \frac{(J_{VI}+D_{VI})}{T_{Ess}*2H} & \alpha_o\left(\frac{(J_{VI}+D_{VI})}{T_{Ess}*2H} - \frac{1}{T_{Ess}}\right) \end{vmatrix} * \begin{vmatrix} \Delta f \\ \Delta P_g \\ \Delta P_d \\ \Delta P_{wind} \\ \Delta P_{Inertia} \end{vmatrix} + \begin{vmatrix} 0 \\ \frac{1}{T_g} \\ 0 \\ 0 \\ 0 \end{vmatrix} * |\Delta P_c| + \begin{vmatrix} 0 & \frac{1}{2H} \\ 0 & 0 \\ 0 & 0 \\ \frac{1}{T_{wind}} & 0 \\ 0 & 0 \\ 0 & \alpha_o\left(\frac{(J_{VI}+D_{VI})}{T_{Ess}*2H}\right) \end{vmatrix} * \begin{vmatrix} \Delta P_{wind} \\ \Delta P_L \end{vmatrix} \tag{9}$$

$$Y = \begin{vmatrix} 1 & 0 & 0 & 0 & 0 \end{vmatrix} * \begin{vmatrix} \Delta f \\ \Delta P_g \\ \Delta P_d \\ \Delta P_{wind} \\ \Delta P_{Inertia} \end{vmatrix} + \begin{vmatrix} 0 & 0 \end{vmatrix} * \begin{vmatrix} \Delta P_{wind} \\ \Delta P_L \end{vmatrix} + |0| * |\Delta P_c| \tag{10}$$

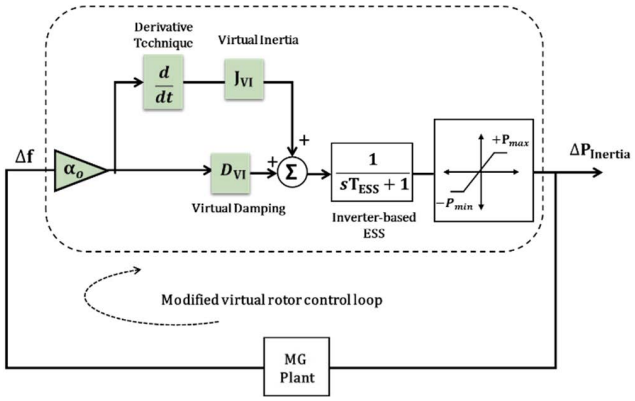

FIGURE 2. The dynamic structure of the modified virtual rotor emulation-based ESS connected to the islanded microgrid.

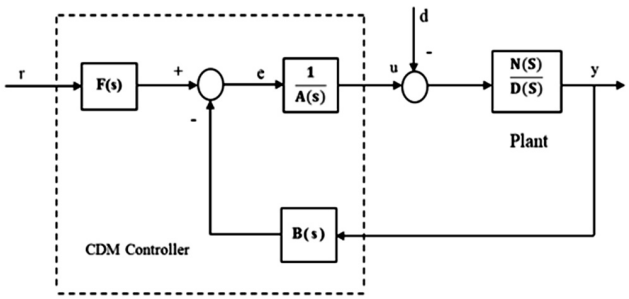

FIGURE 3. Block diagram of CDM control system.

where $P(s)$ can be defined as follow:

$$P(s) = A(s)D(s) + B(s)N(s) \tag{12}$$

where $A(s)$ and $B(s)$ can be calculated as follow:

$$A(s) = \sum_{i=0}^{P} l_i s^i \text{ and } B(s) = \sum_{i=0}^{q} k_i s^i \tag{13}$$

Since l_i and k_i are coefficients of the controller polynomial. The case of $p \geq q$ should be verified for practical considerations.

The actuating signal u for the closed-loop can be defined as:

$$u = \frac{D(s)F(s)}{P(s)}r + \frac{A(s)D(s)}{P(s)}d \tag{14}$$

To acquire the characteristic polynomial $P(s)$, the controller polynomial from Eq. (12) are substituted in Eq. (13) to get:

$$P(s) = \sum_{i=0}^{P} l_i s^i D(s) + \sum_{i=0}^{q} k_i s^i N(s) = \sum_{i=0}^{n} a_i s^i, \quad a_i > 0 \tag{15}$$

Parameters such as the equivalent time constant (τ), the stability indices (γ_i), and the stability limits (γ_i^*) relate to the coefficients of the characteristic polynomial (a_i) as follows:

$$\gamma_i = \frac{a_i^2}{a_{i+i}a_{i-1}}, \quad i \in [1, n-1], \ \gamma_0 = \gamma_n = \infty \tag{16}$$

$$\tau = \frac{a_1}{a_0} \tag{17}$$

$$\gamma_i^* = \frac{1}{\gamma_{i-1}} + \frac{1}{\gamma_{i+1}}, \quad i \in [1, n-1] \tag{18}$$

The value of τ is an important step in the design operation and chosen as:

$$\tau = \frac{t_s}{2.5 \approx 3} \tag{19}$$

According to the standard form of Manabe, γ_i values have been chosen as $\{2.5, 2, 2\ldots2\}$. These values can be changed by the designer. Using τ and γ_i, The target characteristic polynomial, P_{target} can be framed as

$$P_{target} = a_\circ \left[\left\{ \sum_{i=2}^{n} \left(\prod_{j=1}^{i-1} \frac{1}{\gamma_{i-j}^j} \right) (\tau s)^i \right\} + \tau s + 1 \right] \tag{20}$$

where $P(s) = P_{target}(s)$.

Also, the reference numerator polynomials $F(s)$ can be calculated from:

$$F(s) = \frac{(P(s)|_{s=0})}{N(s)} \tag{21}$$

V. GENERAL OVERVIEW OF MULTI-OBJECTIVE SEAGULL AND CLASSIC JAYA ALGORITHMS

A. FOR SEAGULL OPTIMIZER

The multi-objective seagull optimization technique was introduced in [40]. It is an extension of the classic SOA algorithm, with multi-objectivity and search space distinction. It has an archival search space while classic SOA has to do the extra task of providing optimal solutions. Moreover, it has many benefits over classic one such as doesn't need weight factors and usually generate combinations of solutions, allowing computation of an approximation of the entire Pareto front. This algorithm essentially simulates the attacking behavior and migration nature of seagulls. Seagulls are globe-spanning seabirds and are considered very intelligent birds because they have their own strategy (breadcrumbs) to attract prey and make the sound of rain on their feet to attract earthworms hiding underground. The attacking (exploitation) and migration (exploration) strategies of seagulls are their most important behavioral features shown in Fig. 4. Also, they are discussed mathematically and also, and the main steps of the classic and multi-objective SOA are stated in (see [40]). The following three assumptions are made regarding seagulls:

- Seagulls conduct their migration behavior in the form of a swarm. The exact location of each seagull varies to prevent them from colliding into each other.
- Seagulls can move towards the direction of the best seagull in a group. The best seagull indicates the optimal solution with the best value of the fitness function.
- Seagulls always change their location based on their initial position.

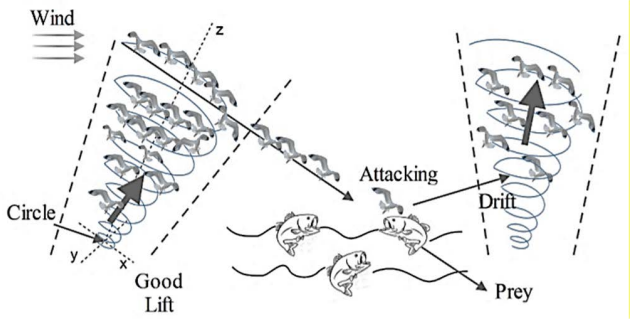

FIGURE 4. Migration and attacking behaviors of seagulls [40].

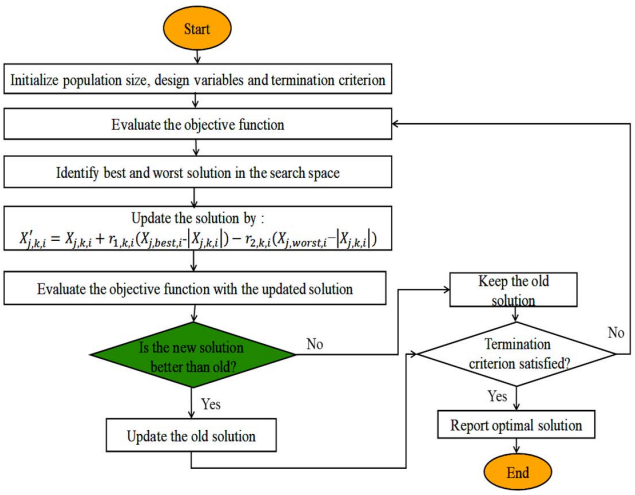

FIGURE 5. Flowchart of the classic Jaya optimizer.

B. FOR STANDARD JAYA OPTIMIZER

Jaya was introduced by Rao in [43]. It does not require adjusting its parameters as compared with other optimizers. The essential precept of the proposed Jaya optimizer is centered around getting the solution by moving towards the best solution and staying away from the worst one. Therefore, its performance is exquisite and powerful, not affected by the wide dimension issue. The procedural steps of the Jaya algorithm are stated in the flowchart shown in Fig. 5.

Jaya algorithm has several benefits such as:

- The issue of selecting the algorithm controller parameters does not exist in this technique
- It can solve unrestricted, restricted issues, and is suitable for discrete optimization problems.
- Plain coding, ease to use, less computational time.
- It is considered more powerful against system uncertainties and variations due to its victorious nature.

VI. JAYA OPTIMIZER BASED BE WITH MODIFIED VIRTUAL ROTOR MECHANISM

Figure 6 shows the addition of the standard Jaya optimizer for adaptive tunning the integral control system supported with the modified virtual rotor control loop. In this technique, only the actual output signal is used to feed the optimizer and it is only utilized to stop the determination in case of lying within a small deviation (about 0.001 pu).

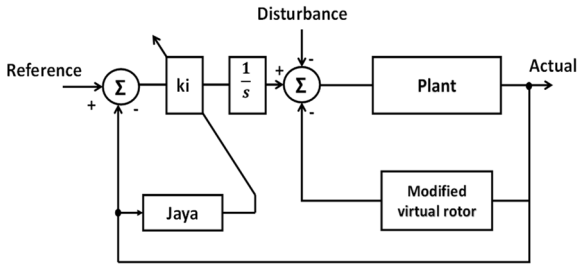

FIGURE 6. Block diagram of the standard Jaya optimizer supported by the modified virtual rotor.

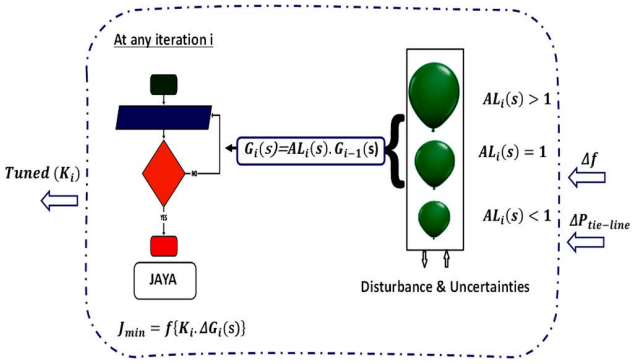

FIGURE 7. Concept of the Balloon Effect at any iteration (i) using Jaya optimizer.

The BE has been added to increment the interactivity of Jaya with the system issues. Figure 7 illustrates the concept of BE. It is noted that the effect of the system problems on $G_i\,(s)$ is like that of air on the balloon volume [32].

The block diagram of the modified virtual rotor and Jaya-based BE for the adaptive control system is shown in Fig. 8.

According to Fig. 8, at any iteration (i), the open-loop transfer function $G_i\,(s)$ can be calculated as:

$$G_i\,(s) = {Y_i(s)}/{U_i(s)} \tag{22}$$

Also $G_i\,(S)$, can be driven using its nominal value $G_0\,(s)$ as:

$$G_i\,(s) = AL_i.G_{i-1}\,(s) \tag{23}$$

where AL_i is the balloon coefficient parameter and

$$G_{i-1}\,(s) = \rho_i.G_0\,(s) \tag{24}$$

where,

$$\rho_i = \prod_{n=1}^{i-1} \mathrm{AL}_n \tag{25}$$

VII. JAYA-BASED ADAPTIVE FREQUENCY REGULATION

The mismatch between seeking real power and generating it at an agreeable frequency causes an issue in load frequency control (LFC). Therefore, BE was introduced based on Jaya optimizer to calculate its effectiveness in resolving these problems within the LFC.

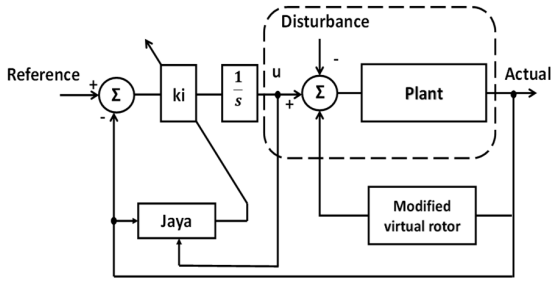

FIGURE 8. Simplified model of studied microgrid-based BE supported adaptive control system with the help of modified virtual rotor.

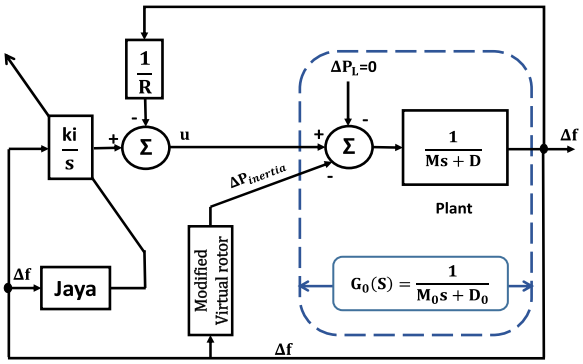

FIGURE 9. General single-area MG block diagram model using classic Jaya and modified virtual rotor.

A. CLASSIC JAYA WITHOUT BALLOON EFFECT

In Fig. 9, there are three control loops used in this work: primary that uses the droop characteristics (1/R) for switching the valve of the governor, secondary that represents in LFC, and tertiary (proposed in this study) for modified virtual rotor mechanism. According to the simplified model of the proposed islanded single area MG with Jaya shown in Fig. 9, the closed-loop transfer function can be calculated as:

$$T.F = \frac{\omega_n^2}{s^{2+2\eta\omega_n s+\omega_n^2}} = \frac{\frac{k_i}{M_o}}{s^2 + \left(\frac{\left(D_o+\frac{1}{R_o}\right)}{M_o}\right)s + \frac{k_i}{M_o}} \tag{26}$$

where D_o, R_o, and M_o are the initial values of D, R, and M, respectively,

$$\omega_n = \sqrt{k_i/M_o} \tag{27}$$

$$\eta = \frac{\left(\frac{\left(D_o+\frac{1}{R_o}\right)}{M_o}\right)}{2.\omega_n} \tag{28}$$

$$T_r = \frac{\pi - \sqrt{(1-\eta^2)}}{\omega_n.\sqrt{(1-\eta^2)}} \tag{29}$$

$$T_s = \frac{4}{\omega_n.\eta} = \frac{8}{\left(\frac{\left(D_o+\frac{1}{R_o}\right)}{M_o}\right)} \tag{30}$$

$$M_p = e^{-\pi\eta/\sqrt{1-\eta^2}} \tag{31}$$

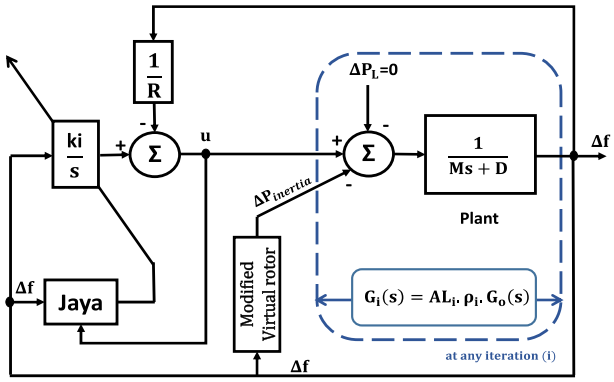

FIGURE 10. Reduced MG model-controlled based BE in the presence of modified virtual rotor.

In this work, the integral square error (ISE) has been chosen as our main objective function (J_{min}) and it could be worded as:

$$J_{min} = \int_0^{t_{sim}} \left((\Delta f)^2 + (\Delta P_{tie-line})^2\right) dt \tag{32}$$

Which is subject to limitations of the I-controller gain as:

$$K_i^{min} \le K_i \le K_i^{max} \tag{33}$$

From Eqs. (22-24), at any iteration (i) it can be noted that (j = f(k$_i$)).

B. CLASSIC JAYA WITH BALLOON EFFECT MODULATION

The reduced linearized model for islanded single area MG using adaptive Jaya-based BE is shown in Fig. 10. From Fig. 10, the actual transfer system function at any iteration (i) can be shaped as:

$$G_i(s) = AL_i.\rho_i.G_o(s) \tag{34}$$

where,

$$G_o(s) = \frac{1}{M_o s + D_o} \tag{35}$$

So, the closed-loop transfer function at any iteration (i) can be computed as:

$$T.F = \frac{\omega_n^2}{s^{2+2\eta\omega_n s+\omega_n^2}} = \frac{\left(\frac{k_i.AL_i.\rho_i}{M_o}\right)}{s^2 + \left(\frac{\left(D_o+\frac{AL_i.\rho_i}{R_o}\right)}{M_o}\right)s + \left(\frac{k_i.AL_i.\rho_i}{M_o}\right)} \tag{36}$$

Then

$$\omega_n = \sqrt{\left(\frac{k_i.AL_i.\rho_i}{M_o}\right)},\ and\ \eta = \frac{\left(\frac{\left(D_o+\frac{AL_i.\rho_i}{R_o}\right)}{M_o}\right)}{2.\omega_n} \tag{37}$$

From Eqs. (34, 35, and 37): at any iteration (i) it can be observed that ($J_{min} = f(k_i, AL_i)$). This supports that the objective function will be affected immediately with AL_i or system changes.

TABLE 1. Description of performance indexes using unimodal and multimodal benchmark test functions.

Function	Formula $f(x)$	Da	Search space	Statistic values	PSO	SOA	Jaya	ESO	Jaya based BE	f_{min}
Sphere (Unimodal)	$\sum_{i=1}^{d}(x_i^2)$	5	[-5,5]	Best	$1.79e^{-08}$	$1.82e^{-016}$	$4.77e^{-14}$	$1.01e^{-15}$	$3.86e^{-18}$	0
				Worst	$1.82e^{-08}$	$1.22e^{-016}$	$4.78e^{-14}$	$1.73e^{-14}$	$3.91e^{-18}$	
				Average error	$6.05e^{-04}$	$1.699e^{-7}$	$3.97e^{-06}$	$8.74e^{-07}$	$5.92\ e^{-08}$	
Rastrigin (Multimodal)	$-10d + \sum_{i=1}^{d}(x_i^2 - 10\cos(2\pi x_i)$	5	[-5,5]	Best	$2.11e^{-09}$	$1.03e^{-15}$	$3.09e^{-09}$	$2.55e^{-13}$	$4.22e^{-18}$	0
				Worst	$1.94e^{-09}$	$8.91e^{-14}$	$3.22e^{-09}$	$2.42e^{-10}$	$3.99e^{-17}$	
				Average error	$2.49e^{-04}$	$3.86e^{-6}$	$3.89e^{-04}$	$5.78e^{-05}$	$1.18\ e^{-07}$	

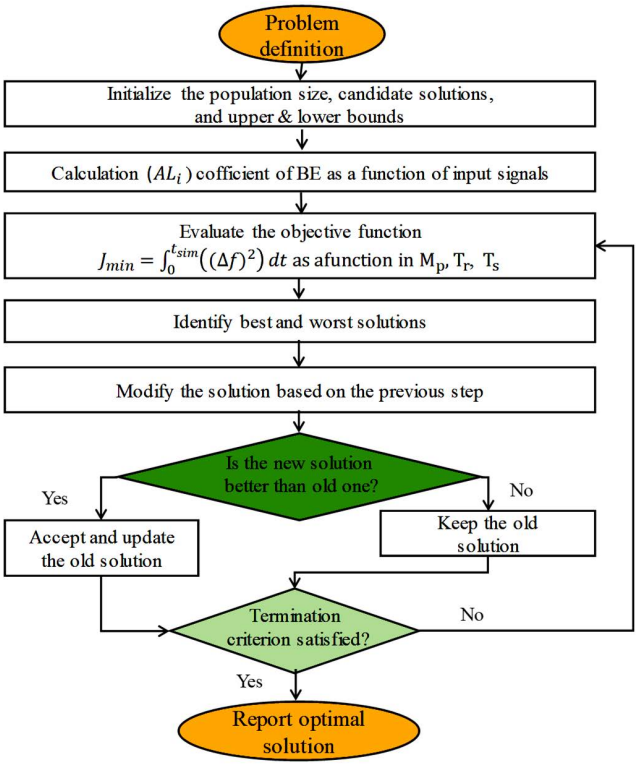

FIGURE 11. Flowchart of the adaptive Jaya optimizer-based BE.

Finally, the procedural steps of the suggested direct adaptive Jaya optimizer based on the BE modulation are constructed in the flowchart as shown in Fig. 11.

VIII. PERFORMANCE ANALYSIS OF THE PROPOSED JAYA BASED BE ON BENCHMARK FUNCTIONS

The effectiveness of the proposed adaptive Jaya-based BE is validated by comparing its performance with other meta-heuristics techniques such as particle swarm (PSO) [29], Electro-search (ESO) [38], multi-objective SOA [40], and classic Jaya algorithms. This validation of the superiority of the Jaya based BE is made into two stages as below:

A. VALIDATION BASED ON A SPEED CONVERGENCE TEST

In this sub-section, a statistical analysis for unimodal (i.e. Sphere) and multimodal (i.e. Rastrigin) benchmark test functions are stated in Table 1. In addition, a comparative analysis to measure the performance and speed convergence of the proposed method compared to standard algorithms such as PSO, Jaya, SOA, and ESO was described. was described. The same number of sets and iterations in each test function was used to solve optimization problems using 20 independent runs performed totally for all of the proposed algorithms and taking 50 as the population size.

It is noted from Table 1 that the proposed adaptive Jaya-based BE converges relatively faster and provides superior to the other algorithms in terms of the best, worst and average error values. Each run stops when the error obtained is less than 10^{-7}.

B. VALIDATION BASED ON THE NON-PARAMETRIC STATISTICAL TEST

In general, non-parametric statistics have not relied on assumptions, i.e. data can be gathered from a pattern that does not put up with a definite distribution.

In this study, pairwise comparisons are used to show the superiority of the proposed adaptive Jaya-based BE compared to standard PSO, ESO, SOA, and Jaya algorithms. In order to apply two algorithms to a common set of problems, these statistical tests are routed for the purpose of comparing them in performance. In this work, the use of the Wilcoxon signed ranks test was introduced [44], as an example of a non-parametric test, due to its simplicity, popularity, safety, and robustness for pairwise comparisons. This section will concentrate on the characterization of Jaya's behavior-based BE, in 1×1 comparisons with the rest of the suggested algorithms mentioned in Table 2.

The Wilcoxon's test is performed as follows: assume d_i be the difference between the two algorithms' performance scores on i^{th} out of n-problems (if it is known that these scores are represented in different ranges, then they can be applied within the interval [0, 1]. The differences are categorized regarding their entire values (for more details see [44]). suppose R^+ is the ranks summation for the problem where the first algorithm superior the second, and R^- is the ranks summation to the reverse. Ranks of $d_i = 0$ are divided equally between the sums assumed using continuous differences d_i;

TABLE 2. Wilcoxon signed-rank test for the objective function performance ISE Of Jaya-based BE with PSO, ESO, SOA, and Jaya.

Comparison	R^+	$R^-/mean$	SD	Z	$p-$Value	$\alpha-$Risk level	Result
Jaya versus PSO	-210	0	53.572	3.9106	6.7860e-08	< 0.05	+
Jaya versus ESO	208	0	53.572	3.8733	1.0473e-06	< 0.05	~
Jaya versus SOA	-92	0	53.572	1.7080	0.06390	> 0.05	–
Jaya based BE versus PSO	82	0	53.549	1.5220	0.06330	> 0.05	–
Jaya based BE versus SOA	210	0	53.549	3.9106	5.7269e-08	< 0.05	+
Jaya based BE versus classic ESO	210	0	53.572	3.9106	5.7269e-08	< 0.05	+
Jaya based BE versus classic Jaya	210	0	53.572	3.9106	2.1917e-07	< 0.05	+

if there is an odd number, one of them is discarded:

$$R^+ = \sum_{d_i<0} rank\,(d_i) + 0.5 \sum_{d_i=0} rank\,(d_i) \tag{38}$$

$$R^- = \sum_{d_i<0} rank\,(d_i) + 0.5 \sum_{d_i=0} rank\,(d_i) \tag{39}$$

From the statistical point of view, this test does not suppose normal distributions and therefore it is considered a safer experience. The first step is to calculate the R^+ and R^- related comparisons between Jaya-based BE and the rest of the algorithms. Once obtained, their associated $p-$values can be stated. Note that, for each comparison, the property $R^+ + R^- = \frac{n\times(n+1)}{2}$ must be true.

Table 2 outlines the $p-$values, R^+, $R^-/mean$, and $\alpha-$risklevel calculated for all the pairwise comparisons concerning Jaya-based BE. It is noted that the adaptive Jaya-based BE shows a worthy enhancement against standard PSO, ESO, SOA, and Jaya algorithms, with a significance level ($\alpha = 0.05$).

The score will be '+' if the control algorithm performs statistically better than the counterpart statically, '−' in the case of the vise verses, and if there are no significant differences found, the result will be '∼'. Where $p-$value is the probability of obtaining a result at least as extreme as the one observed. Moreover, it provides information about whether a statistical hypothesis test is relevant or not and also points out something about how significant the result is: the smaller $p-$value, the stronger the evidence over the null hypothesis. As stated in Table 2, using the standard ESO algorithm shows non-significant improvement over Jaya (meaning there is no difference found '∼').

The final findings indicate that the positive difference ranks summation was greater than the whole negative difference for all scenarios with Jaya-based BE, otherwise, the computed α is much less than the critical value. Thus, this analysis provides extra proof that the proposed adaptive Jaya-based BE algorithm outperforms the other algorithms.

To be more specific, analysis of the variance (ANOVA) test of control performance $J_{min} = ISE_{best}$ obtained by different algorithms are shown in Fig. 12.

TABLE 3. Studied islanded single area MG nominal parameters [13], [32].

Symbol	VALUE	Symbol	VALUE
D	0.12	T_{ESS}	25
H	0.1	J_{VI}	2.5
R	2.4	D_{VI}	1.9
T_g	0.14	P_{max}	0.15
T_t	7	P_{min}	-0.15

TABLE 4. Suggested parameters of the Jaya optimizer.

Parameter	VALUE
No. of search agents	5
No. of iterations (t)	20
Number of design variables	1
The nominal values of (k_i)	[0.10 0.23 0.35 0.40 0.51]
Lower Bound (LB)	-5
Upper Bound (UB)	+5

TABLE 5. Suggested parameters of the Seagull optimizer.

Parameter	VALUE
No. of seagull population	5
No. of iterations (t)	20
Number of design variables	1
Spiral shape correlation constant (u)	1
Spiral shape correlation constant (v)	0.01
Controller of search agent movement behavior (f_c)	2
Spiral radius (r)	RAND [0, 1]
Spiral shape angel (θ)	RAND [0, 2Π)

IX. RESULT AND DISCUSSION

The suggested adaptive Jaya-based BE modulation supported by a modified virtual rotor is used to adjust the LFC of an islanded single area MG system. MATLAB/Simulink software environment is used for validation in this work. The proposed MG system with virtual inertia and virtual damping parameters are included in Table 3. In addition, the nominal parameters for the suggested Jaya and SOA are stated in Table 4 and 5 in a row:

To assess the efficacy of the suggested control strategy (adaptive Jaya-based BE + modified virtual rotor), the

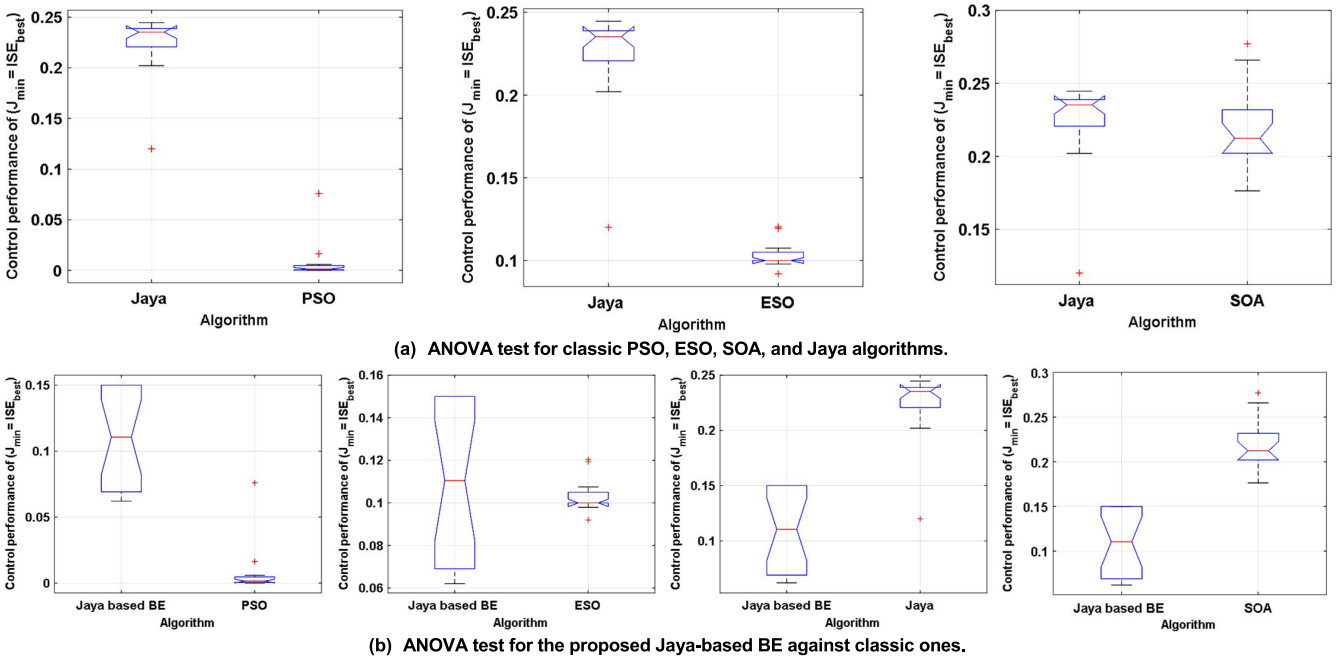

FIGURE 12. ANOVA test of control performance ISE_{best} obtained by different algorithms.

TABLE 6. Performance specification due to a change of 1.5% step load.

Variable	Index	Fixed-I	CDM	SOA	Jaya	Jaya	Jaya based BE	Proposed strategy
						With Virtual inertia		
Δf	Min.	-0.0851	-0.0766	-0.0866	-0.0874	-0.0577	-0.0405	-0.0001
	Max.	0.0639	0.0118	0.0133	0.0173	0.0038	0.0001	0.0039
	Ts	29.361	21.482	18.85	21.074	23.190	20.091	11.359
ΔP_d	Min.	0.00	0.00	0.00	0.00	0.00	0.00	0.00
	Max.	0.0239	0.0166	0.0168	0.0174	0.0155	0.0149	0.0149
	Ts	28.223	19.827	17.68	20.091	23.336	19.990	10.203

proposed single area MG system has been checked into three case studies. The performance specifications: undershoot (Min.), overshoot (Max.), and settling time of the proposed strategy has been presented as numerical evidence for the superiority in performance and compared with multi-objective SOA algorithm, classic Jaya with/without virtual inertia, Jaya based BE with virtual inertia, CDM, and conventional integral controllers.

1) CASE 1: PERFORMANCE ASSESSMENT FOR 1.5% STEP LOAD CHANGE

Here, the studied single area MG system with the introduced coordination method (adaptive Jaya-based BE + modified virtual rotor) is simulated during a step load demand scenario (ΔP_L changes by 0.015 at the time of 3 sec). Figure 13a demonstrates the frequency response of the MG system with common as well as suggested adaptive controllers in this case, similarly in the absence as well as the presence of the proposed modified virtual inertia. It was clear that the MG provides the best performance as well as a higher decline in frequency deviations for adaptive Jaya-based BE modulation (less oscillation and less settling time) as compared to the conventional integral controller, CDM, SOA, and classic Jaya. Moreover, the existence of a modified virtual rotor clearly impacted the system frequency response in the case that it accomplished lessening the undershoot value. Therefore, the MG system with the introduced control strategy can afford the best response (lowest settling time and under/overshoot value Where the deviation in frequency in the case of fixed I-controller, CDM, and adaptive controller tuned by SOA and Jaya optimizers was kept between ± 0.075 Hz, ± 0.044 Hz, ± 0.0301 Hz, and ± 0.035 Hz respectively. Whereas Δf with adaptive Jaya-based BE with modified virtual rotor was kept between ± 0.0016 Hz at the same step load disturbance as shown in Table 6. Consequently, the studied islanded MG frequency response with the suggested adaptive proposed strategy has a lower steady-state error and is better in damping than other ones.

Figure 13b shows the diesel power response in this case of load demand. As shown in Table 6, the proposed system with adaptive Jaya-based BE supported by a modified virtual rotor gives a power change of 0.0149 p.u. It is clear that the system

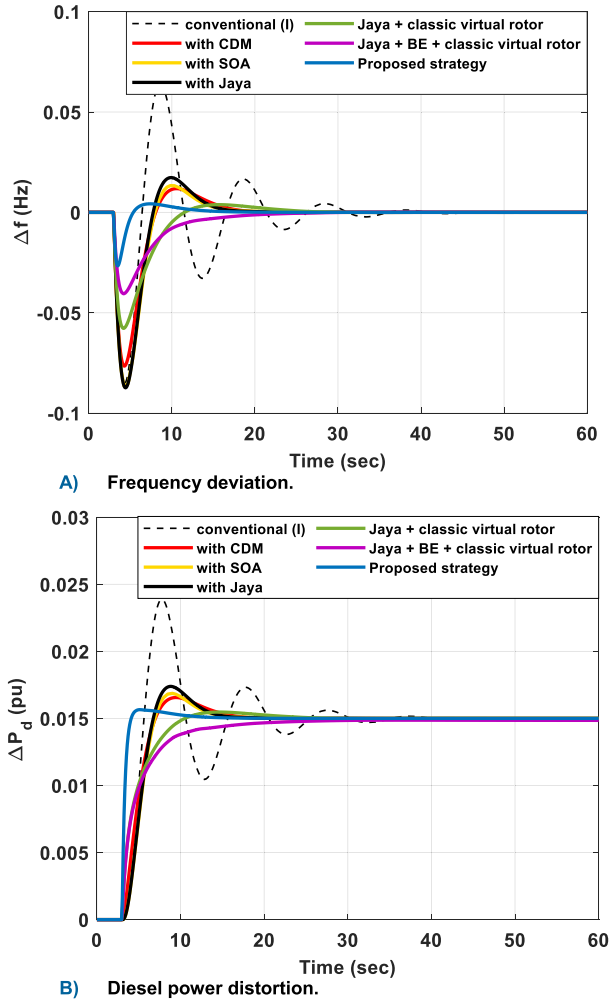

FIGURE 13. System response in case of a step load perturbation.

with the proposed strategy can give preference to diesel power (less settling time) as compared to other ones.

2) CASE 2: PERFORMANCE ASSESSMENT FOR RANDOM LOAD VARIATIONS

On the way to authenticate the MG system with the suggested control system, the MG system is simulated underneath arbitrary load variations. Figure 14 illustrates the trend of arbitrary load demand. It is obvious that from Fig. 14, the load is varied by $+1\%$ at a certain time (20 sec), $+0.5\%$ at 80 sec, afterward reduced by 2% at the time of 150 sec, then -0.5% at the time of 210 sec, while after all stopped at the time of 270 sec. As shown in Fig. 15a, the superior frequency response with fewer over/undershoot is got by means of the introduced control strategy (adaptive Jaya-based BE) intended for online adjusting of the integral controller with the modified virtual rotor as linked to fixed I-controller, CDM, SOA, and classic Jaya with/without virtual inertia controller. Consequently, the planned MG's response with the introduced control scheme is considered to be faster and well-damped than other controllers.

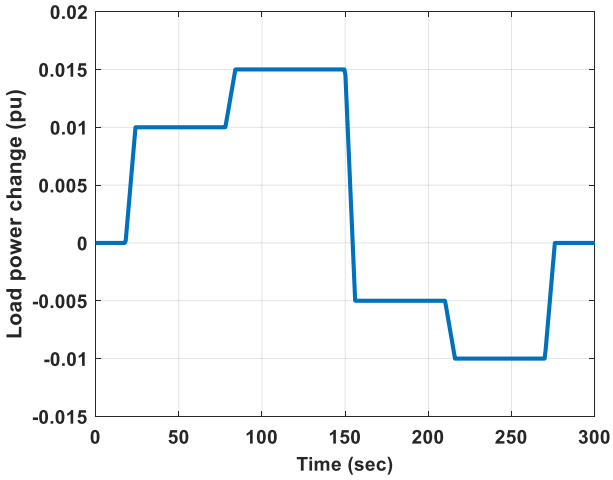

FIGURE 14. Load changes for case 2.

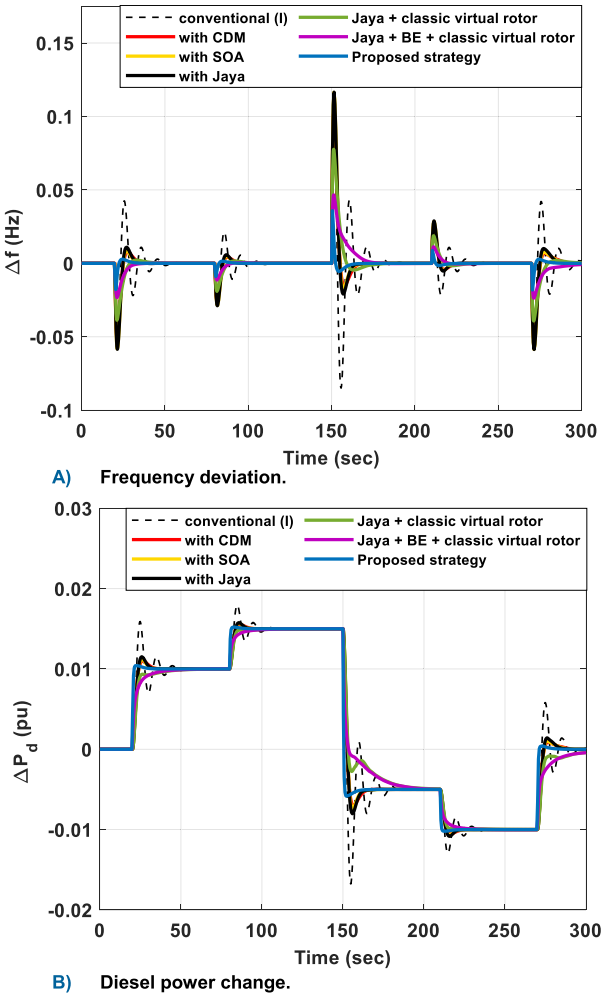

FIGURE 15. System response in case of load variations.

To strengthen the result gained from Fig. 15a, the diesel mechanical power demonstrated in Fig. 15b highlights the predominance of the implied integral controller tuned by the adaptive Jaya-based BE supported by improving virtual rotor.

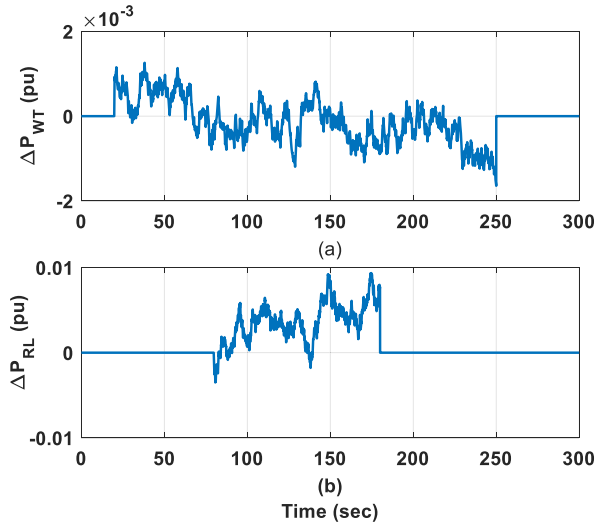

FIGURE 16. Power variations for (a) Wind turbine, (b) Random loads.

3) LAST CASE: PERFORMANCE EVALUATION UNDER PARTIAL INJECTION OF WIND ENERGY AND RANDOM LOAD VARIATIONS

In this study, the performance of the studied islanded single area MG with the proposed control scheme has been tested in face of the uncertainties produced by wind turbine generators and random loads penetrations. The injection of the arbitrary load demand, as well as wind energy, are planned as follows: ΔP_{WT} plugin at the time of 20 sec as well as plug out at 250 sec, ΔP_{RL} plug in at 80 sec, then plug out at the time of 180 sec for a total simulation of 300 sec. Figure 16 indicates the variant shapes of arbitrary demand as well as wind turbine energy.

Figures 17a and 17b illustrate the system response during plug-in/out moments of random loads and wind turbines. A system with an integrated controller adjusted by adaptive Jaya-based BE with the participation of a modified virtual rotor can deal effectively with these variations, whether for frequency or diesel power.

In addition, Fig. 18 demonstrates the interaction between the power change of the virtual rotor and the balloon effect. It is obvious that using adaptive Jaya-based BE in presence of the modified virtual rotor can increase the total amount of inertia power provided to the grid. The positive and negative values indicate the charging/discharging power. Therefore, ESS controlled by the suggested technique is highly charged and discharged in response to any abnormal conditions. Therefore, in the case of high RESs penetration, a fast and stable response can be achieved using the proposed adaptive control strategy.

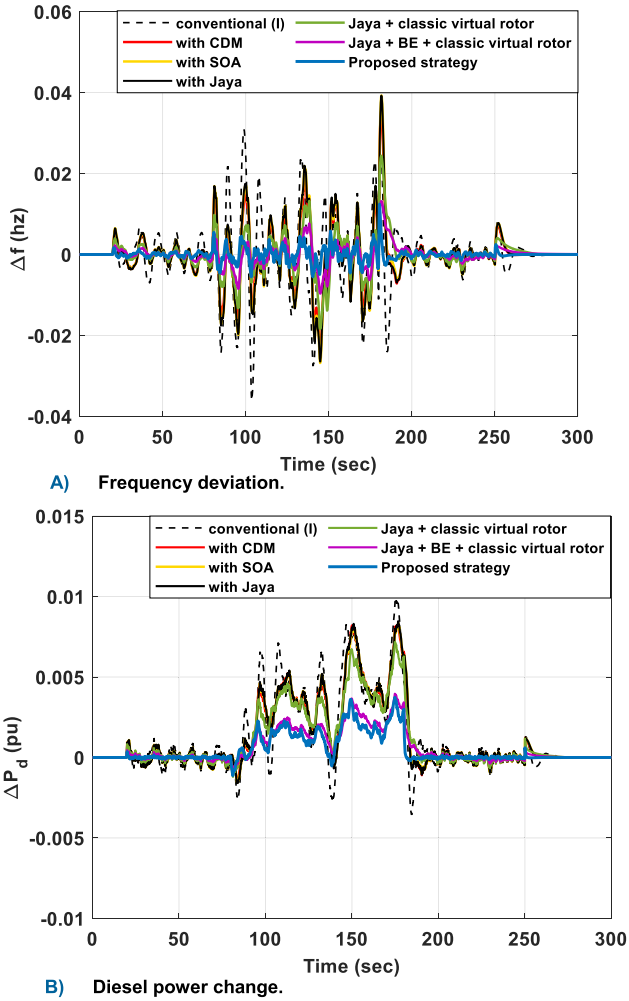

FIGURE 17. System response for the last case.

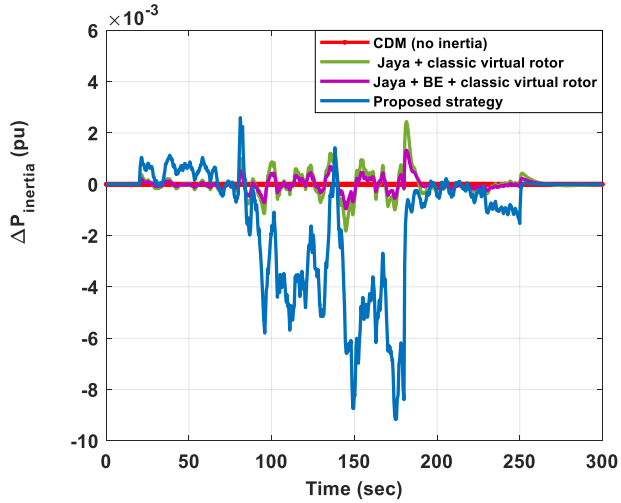

FIGURE 18. Virtual rotor power changes in case of partial injection of wind and demand load power.

X. MULTI-AREA MICROGRID SYSTEM APPLICATION

A. INTERCONNECTED TWO-AREA MICROGRID SYSTEM

The introduced control scheme is expanded to interconnect two areas MGs. It is essential to maintain the power of tie-line $\Delta P_{tieline}$ at the planned values and to rebuild the MG system frequency to its needed level.

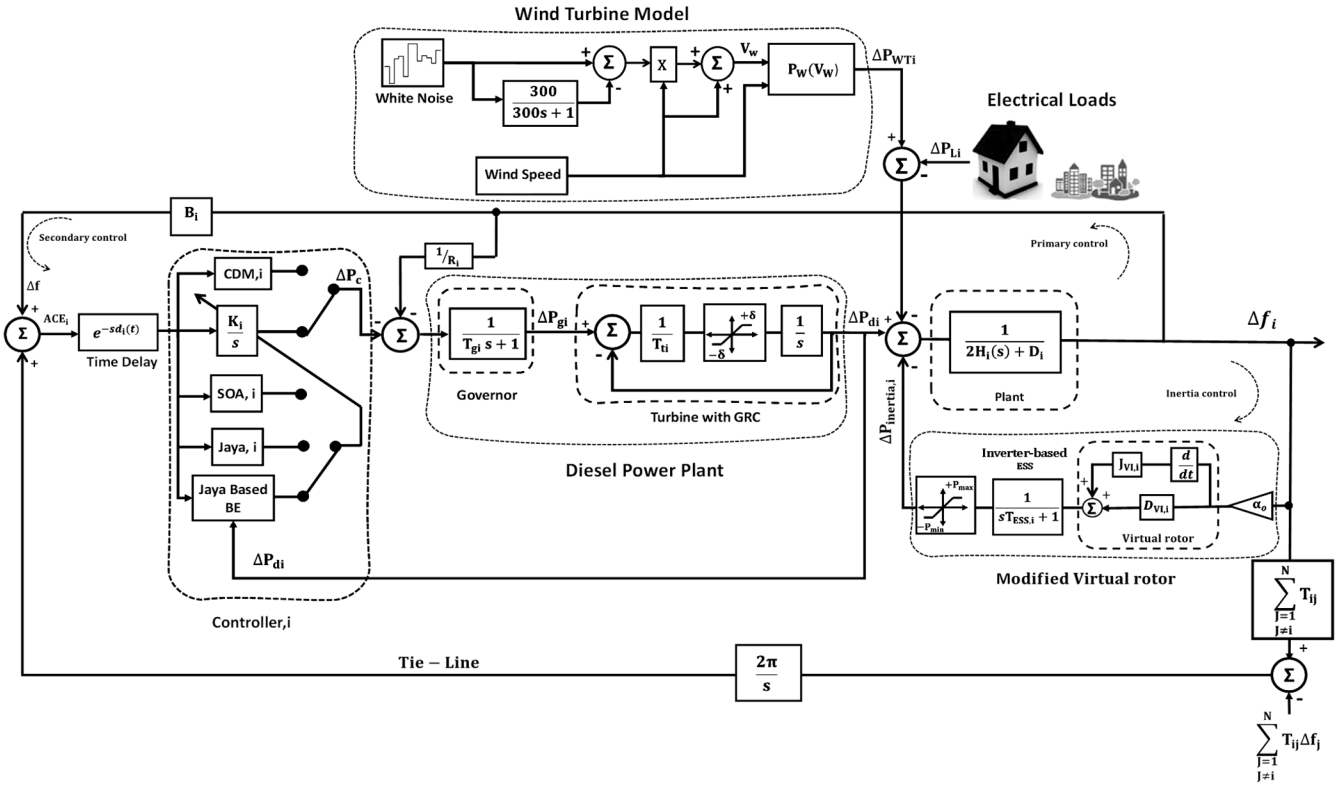

FIGURE 19. Model of the two-area interconnected MG scheme supported by modified virtual rotor.

TABLE 7. Dynamic rated parameters of interconnected two-area MG [13], [36].

Parameter	D_i (pu/Hz)	M_i (pu.sec)	R_i (Hz/pu)	T_{gi} (sec)	T_{ti} (sec)	$T_{ESS,i}$ (sec)	T_{ij} (MW/rad)	β_i (p.u MW/Hz)	$J_{VI,i}$	$D_{VI,i}$	GRC (p.u.MW/min)
Area (1)	0.01	0.1667	3	0.12	0.7	25	$0.565/2\pi$	0.3483	2.5	1.9	10%
Area (2)	0.01	0.2017	2.73	0.12	0.7	14	$0.565/2\pi$	0.3827	1.8	4.8	10%

Digital analyses were achieved to confirm the effectiveness of the introduced coordination control scheme by using adaptive Jaya-based BE modulation carried by a modified virtual rotor (as a tertiary control loop). The nominal data of the introduced two-area MG are defined in Table 7. The simplified model of the interlinked two-area MG is shown in Fig. 19.

The system has been studied and examined under two scenarios through a generation rate constraint (GRC) equal to 10% per minute and 0.05 %. for the highest value of dead band for the governor of every area, along with the communication time delay is supposed to be fixed = 1 second as in [10], [33].

1) SCENARIO 1: PERFORMANCE EVALUATION UNDER THE EFFECT OF A 2.5% STEP LOAD CHANGE

In this scenario, the system is examined under the effect of a 2.5% change in load $\boldsymbol{\Delta P_L}$ at 1 sec. In Figure 20, the deviation in frequency for both areas, diesel power, and the change in tie-line power $\boldsymbol{\Delta P_{tieline}}$ were presented. The system responds with the proposed adaptive Jaya based BE along with modified virtual rotor improved the overall transient MG performance in terms of over/undershoot, settling time, and steady-state error as compared to the fixed (I) controller, CDM, SOA, and classic Jaya with/without virtual inertia in presence of BE. It is noted from Fig. 20d that the change in tie-line power between both areas is effectively enhanced with the proposed control strategy compared to other ones.

As a consequence, this offers a robust indication for the strength of the introduced control scheme over the other relative techniques by enhancing the total transient MG performance as expressed in Table 8.

2) SCENARIO 2: PERFORMANCE EVALUATION UNDER THE EFFECT OF WIND TURBINE AND RANDOM LOADS UNCERTAINTIES

In this study, the change in tie-line power $\Delta P_{tieline}$ and frequency in both areas Δf_1 *and* Δf_2 have been tested under the effect of the injection of wind turbine and loads uncertainties using the same capacity as single area MG in

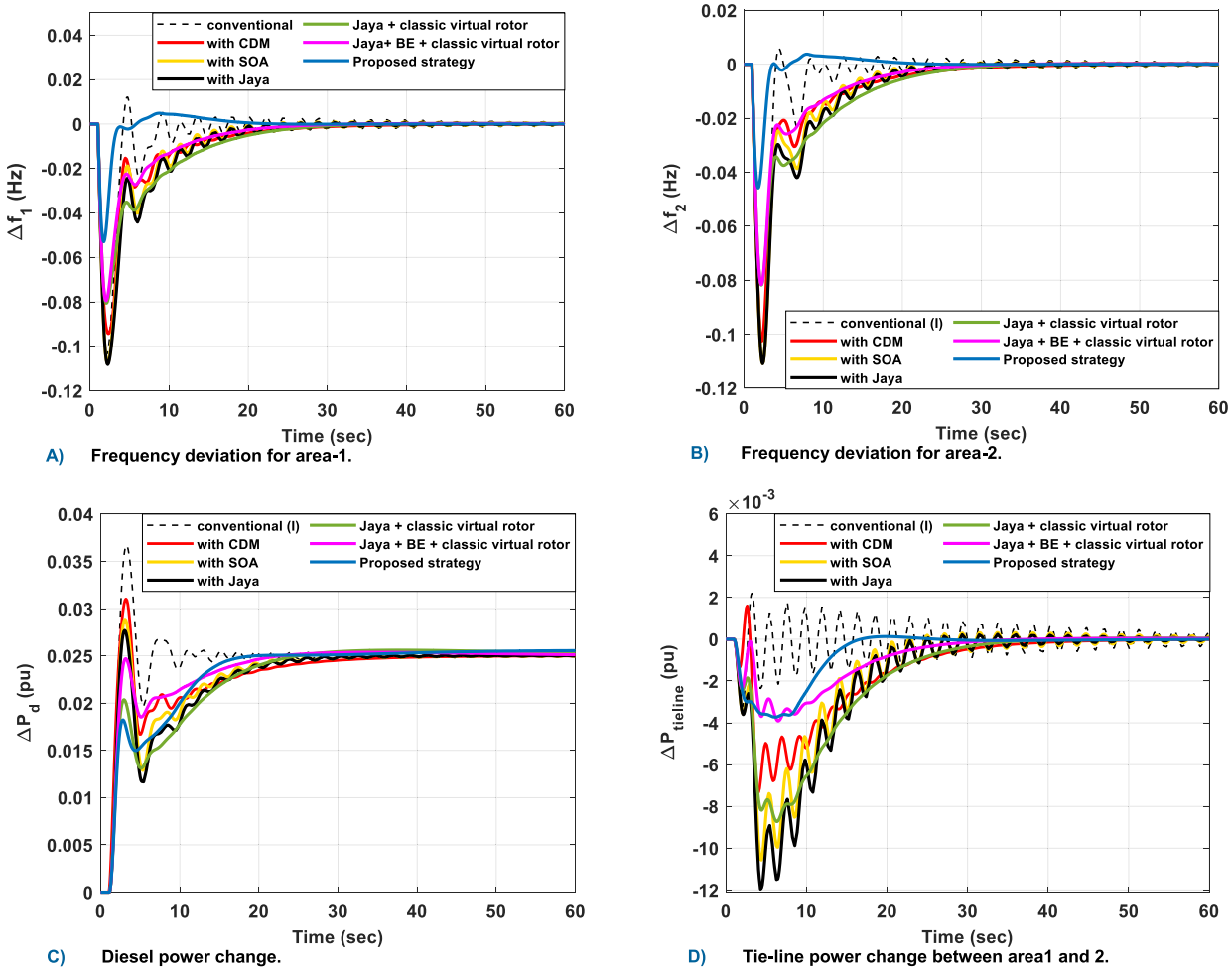

FIGURE 20. System response for scenario-1 in multi-area MGs.

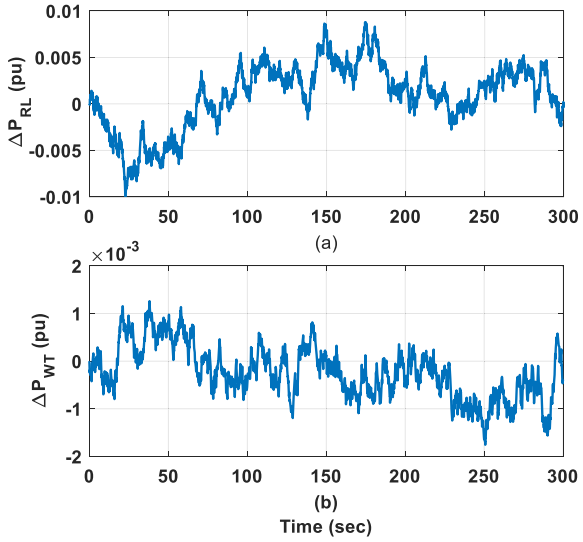

FIGURE 21. Power variations for (a) Random loads, (b) Wind turbine.

this paper. The changes in wind turbine power ΔP_{WT} and loads are shown in Fig. 21.

In Fig. 22, the deviation in the system frequency for SOA, classic Jaya with/without virtual inertia, conventional integral, and CDM controllers reaches an unacceptable value, which leads to system collapse and instability. In contrast, the proposed coordination strategy (adaptive Jaya-based BE + modified virtual rotor) provides superior performance when successfully treating this contingency.

In addition, the power change in the tie-line power as indicated in Fig. 22d is effectively improved to support the superiority of the proposed online tuned (adaptive Jaya-based BE) controller supported by a modified virtual rotor as compared to other ones.

In Fig. 23, it is clear that using adaptive Jaya-based BE modulation in presence of the modified virtual rotor can increase the total amount of inertia power supported to the MGs. It is obvious that the ESS controlled by the suggested technique is highly charged and discharged in response to any abnormal conditions. Therefore, in the case of high RESs penetration, larger participation can be achieved using the proposed adaptive control strategy.

B. SPECIAL CASE STUDY: SYSTEM ASSESSMENT CONSIDERING TIME-VARYING DELAY

To demonstrate the stability of the dynamical system, Lyapunov–Krasovskii functional (LKF) is one of the most

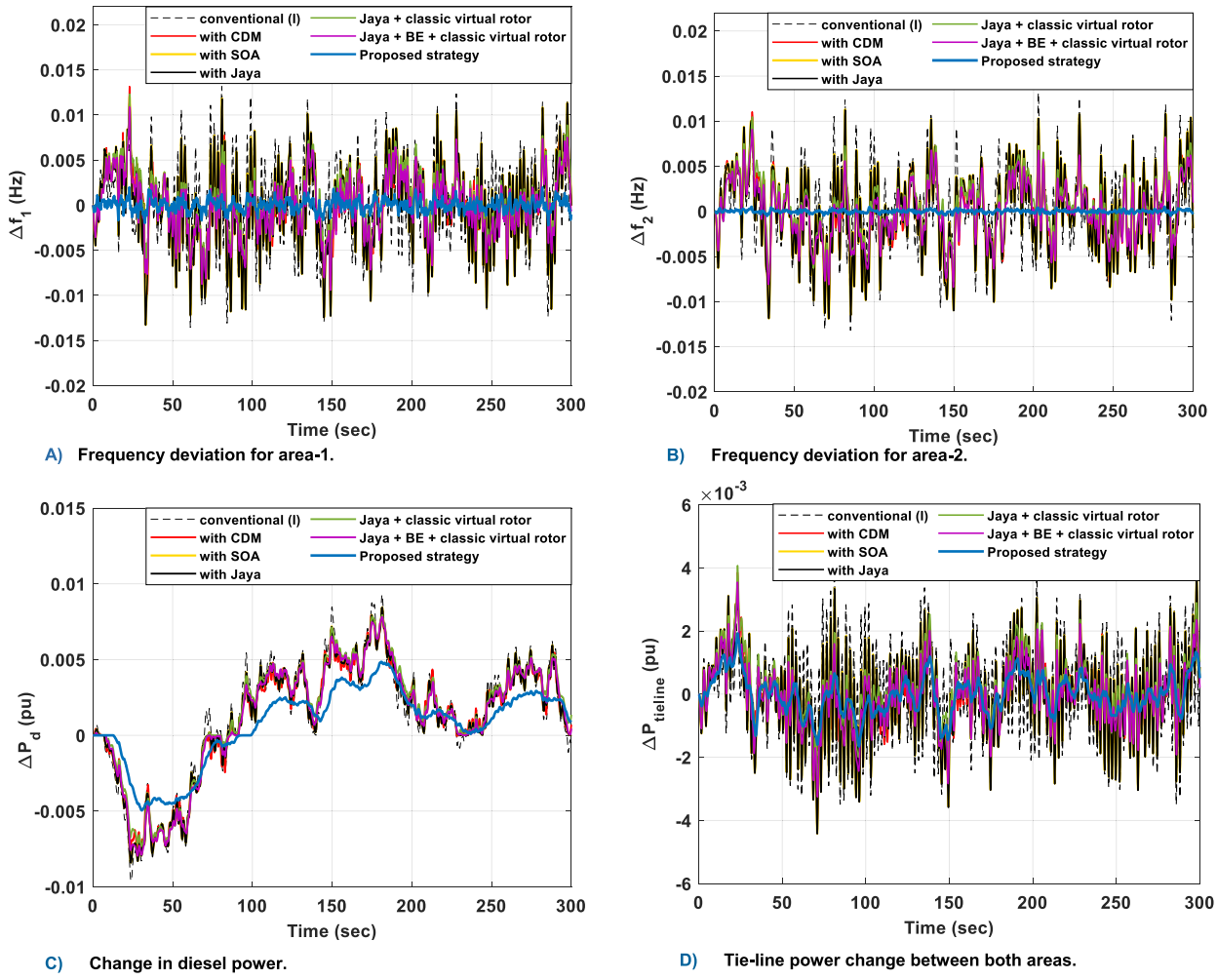

FIGURE 22. System response for scenario-2 in multi-area MGs.

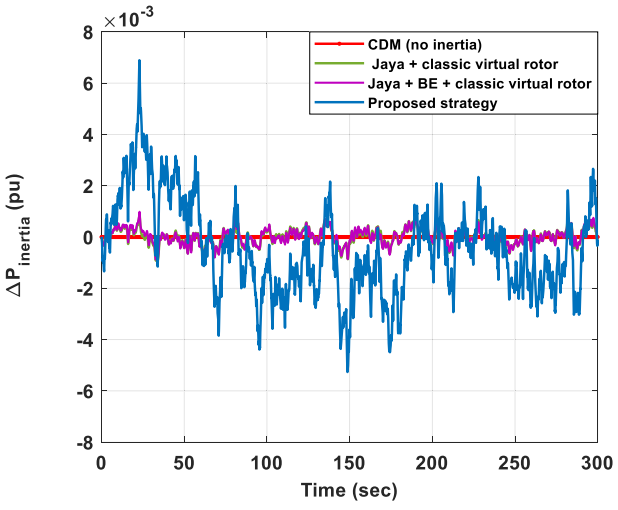

FIGURE 23. Virtual rotor power changes in case of full wind and load power injection.

working techniques, in which terms for stability analysis are derived in terms of linear matrix inequality (LMIs) [27].

Figure 19 shows the linearized model of multi-area MGs with time-varying delays (the i^{th} control area ($i = 1, 2, \ldots, N$)). The state-space representation is given below:

$$\begin{aligned} \dot{x}(t) &= Ax(t) + Bu(t) + \bar{F}\Delta P_L \\ &= Ax(t) + A_d(t - d(t)) \end{aligned} \tag{40}$$

$$y(t) = Cx(t) \tag{41}$$

where $0 < d(t) \leq h$ and:

$$x_i(t) = \left[\Delta f_i \Delta P_{gi} \Delta P_{di} \Delta P_{WTi} \Delta P_{Inertia,i} \int ACE_i \Delta P_{tie-line,i}\right] \tag{42}$$

$$y_i(t) = \left[ACE_i \int_o^t ACE_i(s)\, ds\right] \tag{43}$$

For more details on matrices and state vectors $u(t)$, $B(t)$, A, B, and C (see [27], [28]).

As reported in the literature survey, we observed that an increment of (K_i) affects a less stable LFC system and may affect a notable mimicking in delay margins. To check

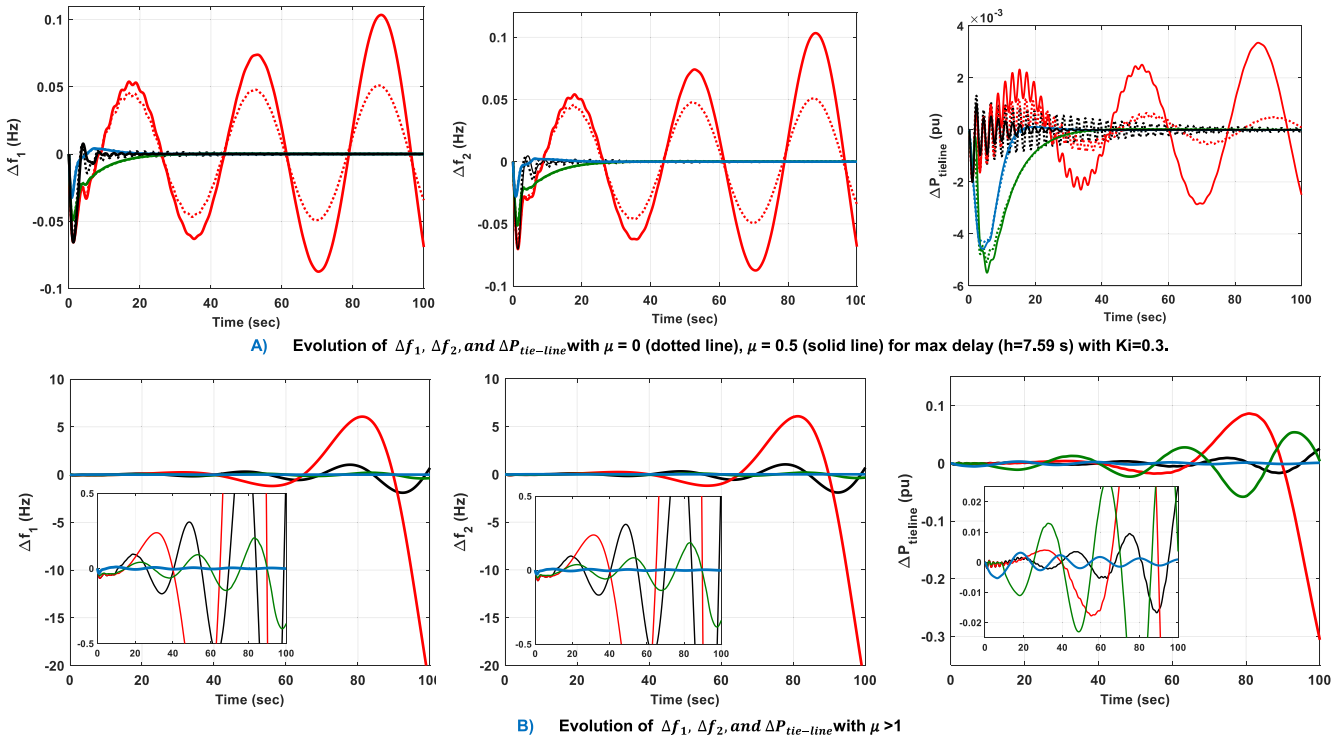

FIGURE 24. System dynamic response due to time-varying communication delay. Solid/dotted lines represent: (Black → conventional ki), (Red→CDM), (Green→ adaptive optimizer), and (Blue→ proposed method).

TABLE 8. Performance specification due to a change of 2.5% step load for multi-area MGs.

Variable	Index	Fixed-I	CDM	SOA	Classic Jaya	Jaya + virtual inertia	Jaya based BE + virtual inertia	Proposed strategy
Δf_1	Min.	-0.1035	-0.0942	-0.1077	-0.1082	-0.0806	-0.0795	-0.0529
	Max.	0.0121	0.000	0.0009	0.0007	0.0003	0.0002	0.0041
	Ts	> 60	33.05	53.42	55.57	36.68	33.81	21.44
Δf_2	Min.	-0.1098	-0.1026	-0.1108	-0.1110	-0.0818	-0.0817	-0.0458
	Max.	0.0058	0.00	0.0007	0.0005	0.0003	0.0002	0.0030
	Ts	> 60	31.75	51.81	54.80	37.126	33.81	21.81
ΔP_d	Min.	0.00	0.000	0.000	0.000	0.000	0.000	0.000
	Max.	0.0367	0.0311	0.0289	0.0277	0.0247	0.0203	0.0182
	Ts	46.045	31.92	30.45	36.76	25.39	23.51	18.53
$\Delta P_{tieline}$	Min.	-0.0032	0.0311	-0.0106	-0.0120	-0.0087	-0.0039	-0.0037
	Max.	0.0022	0.0016	0.0003	0.0002	$5.4e^{-5}$	$3.9e^{-5}$	0.0001
	Ts	> 60	51.57	38.80	40.55	36.45	32.26	21.53

the stable delay margins correctness, time-domain simulations were carried out in Fig. 24 using Matlab/Simulink R2021a.

In this particular study, we tested the proposed interconnected MG in case of $0 \leq \mu > 1$ for the maximum delay of 7.59 in case of ($K_i = 0.3$) fixed/tuned by the proposed Jaya-based BE modulation. The main target is to demonstrate maximum upper bound and get less conservation.

Moreover, graphical results of deviation variables $\Delta f_1, \Delta f_2,$ *and* $\Delta P_{tie-line}$ are shown in Fig. 24 with consideration of fixed/adaptive sets of I-controller. It is observed from Fig 24a that the evolution of $\Delta f_1, \Delta f_2,$ *and* $\Delta P_{tie-line}$ for the interconnected MGs model is asymptotically stable for $h = 7.59$ s (Max. delay upper bound), and $\mu = 0$ and 0.5, $K_i = 0.3$ for each of the controlled areas.

The final finding regarding this special case study of the suggested MG model becomes stable in the case of the proposed direct adaptive Jaya-based BE modulation within $0 \leq \mu > 1$. In addition. It becomes unstable for the other proposed controllers if the delay is exceeding the derived upper bounds for all cases of $\mu > 1$. Therefore, it can be easily seen that the upper bound of the delay is increased beyond the derived upper bound, the system turns into unstable nature as shown in Fig. 24b for CDM controller (which can't handle the delay for all suggested cases) and conventional integral controller and classic optimizers which

start to increase until fall into the unstable region due to the incremental in μ by time.

XI. CONCLUSION

This paper investigates a new coordination strategy for solving LFC issues in islanded single and interconnected areas MGs. The help of using optimization techniques is appeared in this study using multi-objective seagull and Jaya optimizers. The concept of the direct adaptive control has been introduced with Jaya optimizer-based BE modulation for frequency and tie-line power flow regulations considering a modified virtual rotor (virtual inertia + virtual damping) considering full participation of inverter-based ESS (100%) as a tertiary controller within both MGs to dampen the oscillations in the system. The entire balloon effect concept is designed to sense a plant's input and output signals to determine the actual transfer function at each iteration (i). Therefore, this aid increases the efficiency of the Jaya algorithm to deal with system difficulties. The main purpose of using a modified mechanism of the virtual rotor is to emulate the reduction in system inertia and the enhanced damping properties by taking into account the participation of inverter-based ESS. A performance comparative study between the proposed coordination strategy (direct adaptive Jaya-based BE modulation with the modified virtual rotor), conventional integral controller, coefficient diagram method, multi-objective seagull optimizer, and classic Jaya with/without virtual inertia controller is performed for islanded single-area and interconnected two-area MGs. It is obvious that the proposed scheme can be effectively applied to the studied MGs for online tuning of the integral secondary controller gain to minimize the deviations in the system frequency and regulate the power in the tie-line. For superiority of the proposed method, a non-parametric statistics analysis was carried out to prove the effectiveness of the proposed method against other standard metaheuristics algorithms (i.e. PSO, ESO, and SOA) and classic Jaya algorithms. This validation was supported with the speed convergence test and analysis in variance ANOVA. The final findings emphasized the effectiveness of the proposed scheme in comparison to other controllers. In addition, it has achieved effective performance and stability during high perturbations of load demands and penetrations of wind generators. In addition, it proved that the direct adaptive Jaya-based balloon effect significantly outperforms other algorithms in terms of solution quality, convergence speed, and robustness, especially for unimodal and multimodal functions. Additionally, the non-parametric statistical test confirmed that the optimality of solutions was enriched significantly.

Drawbacks, Limitations, and Future Works:

i. The proposed algorithm has still been applied to small-scale optimization problems (<100 design variables).
ii. Additionally, we do not actually know which objective functions we wish to optimize since they rely on the behaviour of the running model. Therefore, we gather information about the objective function from past observations and use that knowledge to optimize it.
iii. Absence of the online tunning for the proposed virtual inertia and virtual damping coefficient parameters.

For future works: This coordination concept can be extended in several applications such as Self-adaptive tuning of virtual rotor parameters, and Grid-forming converters applications based on the hierarchical control strategy for large-scale power plants.

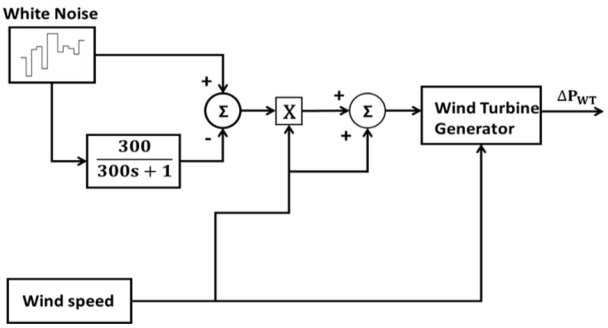

FIGURE 25. Model of wind power generation.

APPENDIX

A. POWER GENERATION OF WIND

A simplified white noise-based wind power generation model is shown in Fig. 25 to obtain a precise output power profile in the renewable sources and random speeds that are adjusted by the white mass noise using MATLAB software environment that is duplicated by the initial speed of the wind. The arithmetic equations for the wind energy system can be depicted as follows:

$$P_w = 0.5\rho A_T V_m^3 C_P(\lambda, \beta) \tag{A.1}$$

where A_T is the area of rotor sweep (m^2), ρ is the density of air (kg/m3), V_m is the wind speed (m/s) (rated), and C_P is the rotor blade's power coefficient. β is the pitch angle and it is defined below in terms of turbine coefficient $C_1 - C_7$.

$$C_P(\lambda, \beta) = C_1 \times \left(\frac{C_2}{\lambda_1} - C_3\beta - C_3\beta^2 - C_5\right) \times e^{-C_6/\lambda_1} + C_7\lambda_T \tag{A.2}$$

where λ_T corresponds to the optimal tip-speed ratio (TSR) and is defined by the following equation:

$$\lambda_T = \left(\frac{W_T * r_T}{V_m}\right) \tag{A.3}$$

where r_T is the rotor radius.

B. RANDOM LOAD MODEL

In [10], illustrates more details about the random load simplified model that is suggested in this research. In this model, the load deviation is simulated close to an actual load change by the following function:

$$\Delta \boldsymbol{P}_{\boldsymbol{Load}} = 0.6\sqrt{\Delta \boldsymbol{P}_{\boldsymbol{Load}}} \tag{A.4}$$

DECLARATION OF COMPETING INTEREST

The authors declare no conflicts of interest concerning this work.

REFERENCES

[1] J. A. P. Lopes, C. L. Moreira, and A. G. Madureira, "Defining control strategies for microgrids islanded operation," *IEEE Trans. Power Syst.*, vol. 21, no. 2, pp. 916–924, May 2006, doi: 10.1109/TPWRS.2006.873018.

[2] D. Emara, M. Ezzat, A. Y. Abdelaziz, K. Mahmoud, M. Lehtonen, and M. M. F. Darwish, "Novel control strategy for enhancing microgrid operation connected to photovoltaic generation and energy storage systems," *Electronics*, vol. 10, no. 11, p. 1261, May 2021, doi: 10.3390/ELECTRONICS10111261.

[3] K. T. Tan, P. L. So, Y. C. Chu, and M. Z. Q. Chen, "A flexible AC distribution system device for a microgrid," *IEEE Trans. Energy Convers.*, vol. 28, no. 3, pp. 601–610, Sep. 2013, doi: 10.1109/TEC.2013.2260162.

[4] D. E. Olivares, A. Mehrizi-Sani, A. H. Etemadi, C. A. Cañizares, R. Iravani, M. Kazerani, A. H. Hajimiragha, O. Gomis-Bellmunt, M. Saeedifard, R. Palma-Behnke, G. A. Jiménez-Estévez, and N. D. Hatziargyriou, "Trends in microgrid control," *IEEE Trans. Smart Grid*, vol. 5, no. 4, pp. 1905–1919, Jul. 2014, doi: 10.1109/TSG.2013.2295514.

[5] A. K. Barik and D. C. Das, "Integrated resource planning in sustainable energy-based distributed microgrids," *Sustain. Energy Technol. Assessments*, vol. 48, Dec. 2021, Art. no. 101622, doi: 10.1016/J.SETA.2021.101622.

[6] A. S. Abbas, R. A. El-Sehiemy, A. A. El-Ela, E. S. Ali, K. Mahmoud, M. Lehtonen, and M. M. F. Darwish, "Optimal harmonic mitigation in distribution systems with inverter based distributed generation," *Appl. Sci.*, vol. 11, no. 2, p. 774, Jan. 2021, doi: 10.3390/APP11020774.

[7] H. Abubakr, J. C. Vasquez, K. Mahmoud, M. M. F. Darwish, and J. M. Guerrero, "Comprehensive review on renewable energy sources in egypt—Current status, grid codes and future vision," *IEEE Access*, vol. 10, pp. 4081–4101, 2022, doi: 10.1109/ACCESS.2022.3140385.

[8] S. Grillo, V. Musolino, L. Piegari, E. Tironi, and C. Tornelli, "DC islands in AC smart grids," *IEEE Trans. Power Electron.*, vol. 29, no. 1, pp. 89–98, Jan. 2014, doi: 10.1109/TPEL.2013.2251666.

[9] M. Corti, G. Superti-Furga, E. Tironi, A. M. Pavan, and G. Sulligoi, "Intentional islanding in medium voltage distribution grids," in *Proc. IEEE 16th Int. Conf. Environ. Electr. Eng. (EEEIC)*, Jun. 2016, pp. 1–6, doi: 10.1109/EEEIC.2016.7555675.

[10] H. Abubakr, T. H. Mohamed, M. M. Hussein, J. M. Guerrero, and G. Agundis-Tinajero, "Adaptive frequency regulation strategy in multi-area microgrids including renewable energy and electric vehicles supported by virtual inertia," *Int. J. Electr. Power Energy Syst.*, vol. 129, Jul. 2021, Art. no. 106814, doi: 10.1016/j.ijepes.2021.106814.

[11] A. Fawzy, A. Bakeer, G. Magdy, I. E. Atawi, and M. Roshdy, "Adaptive virtual inertia-damping system based on model predictive control for low-inertia microgrids," *IEEE Access*, vol. 9, pp. 109718–109731, 2021, doi: 10.1109/ACCESS.2021.3101887.

[12] T. Kerdphol, F. S. Rahman, M. Watanabe, Y. Mitani, D. Turschner, and H. P. Beck, "Enhanced virtual inertia control based on derivative technique to emulate simultaneous inertia and damping properties for microgrid frequency regulation," *IEEE Access*, vol. 7, pp. 14422–14433, 2019, doi: 10.1109/access.2019.2892747.

[13] H. Abubakr, J. M. Guerrero, and J. C. Vasquez, "Modified virtual inertia mechanism based ESS for a real multi-source power system application: The Egyptian grid," in *Proc. 47th Annu. Conf. IEEE Ind. Electron. Soc. (IECON)*, Oct. 2021, pp. 1–6, doi: 10.1109/IECON48115.2021.9589898.

[14] E. Rakhshani and P. Rodriguez, "Inertia emulation in AC/DC interconnected power systems using derivative technique considering frequency measurement effects," *IEEE Trans. Power Syst.*, vol. 32, no. 5, pp. 3338–3351, Sep. 2017, doi: 10.1109/TPWRS.2016.2644698.

[15] P. Saxena, N. Singh, and A. K. Pandey, "Enhancing the dynamic performance of microgrid using derivative controlled solar and energy storage based virtual inertia system," *J. Energy Storage*, vol. 31, Oct. 2020, Art. no. 101613, doi: 10.1016/J.EST.2020.101613.

[16] S. K. Bhagat, L. C. Saikia, N. R. Babu, and D. Saha, "Impact of PLL and virtual inertia on deregulated AGC system integrated with parallel AC/HVDC," *IETE J. Res.*, vol. 67, no. 1, pp. 1–14, Mar. 2021, doi: 10.1080/03772063.2021.1894249.

[17] B. Long, Y. Liao, K. T. Chong, J. Rodriguez, and J. M. Guerrero, "Enhancement of frequency regulation in AC microgrid: A fuzzy-MPC controlled virtual synchronous generator," *IEEE Trans. Smart Grid*, vol. 12, no. 4, pp. 3138–3149, Jul. 2021, doi: 10.1109/TSG.2021.3060780.

[18] B. Alghamdi and C. Cañizares, "Frequency and voltage coordinated control of a grid of AC/DC microgrids," *Appl. Energy*, vol. 310, Mar. 2022, Art. no. 118427, doi: 10.1016/J.APENERGY.2021.118427.

[19] H. Abubakr, J. C. Vasquez, T. H. Mohamed, and J. M. Guerrero, "The concept of direct adaptive control for improving voltage and frequency regulation loops in several power system applications," *Int. J. Electr. Power Energy Syst.*, vol. 140, Sep. 2022, Art. no. 108068, doi: 10.1016/j.ijepes.2022.108068.

[20] M. Elsisi, K. Mahmoud, M. Lehtonen, and M. M. F. Darwish, "Effective nonlinear model predictive control scheme tuned by improved NN for robotic manipulators," *IEEE Access*, vol. 9, pp. 64278–64290, 2021, doi: 10.1109/ACCESS.2021.3075581.

[21] A. M. Othman and A. A. El-Fergany, "Design of robust model predictive controllers for frequency and voltage loops of interconnected power systems including wind farm and energy storage system," *IET Gener. Transmiss. Distrib.*, vol. 12, no. 19, pp. 4276–4283, Oct. 2018, doi: 10.1049/IET-GTD.2018.5568.

[22] G. Sharma, A. Panwar, Y. Arya, and M. Kumawat, "Integrating layered recurrent ANN with robust control strategy for diverse operating conditions of AGC of the power system," *IET Gener., Transmiss. Distrib.*, vol. 14, no. 18, pp. 3886–3895, Sep. 2020, doi: 10.1049/IET-GTD.2019.0935.

[23] Y. Arya, N. Kumar, P. Dahiya, G. Sharma, E. Çelik, S. Dhundhara, and M. Sharma, "Cascade-$I^{\lambda}D^{\mu}N$ controller design for AGC of thermal and hydro-thermal power systems integrated with renewable energy sources," *IET Renew. Power Gener.*, vol. 15, no. 3, pp. 504–520, Feb. 2021, doi: 10.1049/RPG2.12061.

[24] H. Ali, G. Magdy, B. Li, G. Shabib, A. A. Elbaset, D. Xu, and Y. Mitani, "A new frequency control strategy in an islanded microgrid using virtual inertia control-based coefficient diagram method," *IEEE Access*, vol. 7, pp. 16979–16990, 2019, doi: 10.1109/access.2019.2894840.

[25] M. E. C. Bento, "Fixed low-order wide-area damping controller considering time delays and power system operation uncertainties," *IEEE Trans. Power Syst.*, vol. 35, no. 5, pp. 3918–3926, Sep. 2020, doi: 10.1109/TPWRS.2020.2978426.

[26] L. Jiang, W. Yao, Q. H. Wu, J. Y. Wen, and S. J. Cheng, "Delay-dependent stability for load frequency control with constant and time-varying delays," *IEEE Trans. Power Syst.*, vol. 27, no. 2, pp. 932–941, May 2012, doi: 10.1109/TPWRS.2011.2172821.

[27] S. Arunagirinathan and P. Muthukumar, "New asymptotic stability criteria for time-delayed dynamical systems with applications in control models," *Results Control Optim.*, vol. 3, Jun. 2021, Art. no. 100014, doi: 10.1016/J.RICO.2021.100014.

[28] F. Yang, J. He, J. Wang, and M. Wang, "Auxiliary-function-based double integral inequality approach to stability analysis of load frequency control systems with interval time-varying delay," *IET Control Theory Appl.*, vol. 12, no. 5, pp. 601–612, Mar. 2018, doi: 10.1049/IET-CTA.2017.1187.

[29] T. H. Mohamed, H. Abubakr, M. M. Hussein, and G. S. Salman, "Adaptive load frequency control in power systems using optimization techniques," in *AI and Learning Systems—Industrial Applications and Future Directions*. London, U.K.: IntechOpen, 2021, pp. 201–215.

[30] M. N. Ali, M. Soliman, K. Mahmoud, J. M. Guerrero, M. Lehtonen, and M. M. F. Darwish, "Resilient design of robust multi-objectives PID controllers for automatic voltage regulators: D-decomposition approach," *IEEE Access*, vol. 9, pp. 106589–106605, 2021, doi: 10.1109/ACCESS.2021.3100415.

[31] G. Sharma, N. Krishnan, Y. Arya, and A. Panwar, "Impact of ultracapacitor and redox flow battery with Jaya optimization for frequency stabilization in linked photovoltaic-thermal system," *Int. Trans. Electr. Energy Syst.*, vol. 31, no. 5, p. e12883, May 2021, doi: 10.1002/2050-7038.12883.

[32] H. Abubakr, J. M. Guerrero, J. C. Vasquez, and T. H. Mohamed, "A novel modulation for adaptive control issue-based optimization techniques: Balloon effect," in *Proc. 22nd Int. Middle East Power Syst. Conf. (MEPCON)*, Dec. 2021, pp. 412–415, doi: 10.1109/MEPCON50283.2021.9686253.

[33] Y. A. Dahab, H. Abubakr, and T. H. Mohamed, "Adaptive load frequency control of power systems using electro-search optimization supported by the balloon effect," *IEEE Access*, vol. 8, pp. 7408–7422, 2020, doi: 10.1109/ACCESS.2020.2964104.

[34] M. Č. Bošković, T. B. Šekara, and M. R. Rapaić, "Novel tuning rules for PIDC and PID load frequency controllers considering robustness and sensitivity to measurement noise," *Int. J. Electr. Power Energy Syst.*, vol. 114, Jan. 2020, Art. no. 105416, doi: 10.1016/J.IJEPES.2019.105416.
[35] E. Çelik, N. Öztürk, Y. Arya, and C. Ocak, "(1 + PD)-PID cascade controller design for performance betterment of load frequency control in diverse electric power systems," *Neural Comput. Appl.*, vol. 33, no. 22, pp. 15433–15456, Jun. 2021, doi: 10.1007/S00521-021-06168-3.
[36] H. Abubakr, M. M. Hussein, and T. H. Mohamed, "Frequency stabilization of two area power system interconnected by AC/DC links using Jaya algorithm," *Int. J. Adv. Sci. Technol.*, vol. 29, no. 1, pp. 548–559, 2020.
[37] M. H. Fini, G. R. Yousefi, and H. H. Alhelou, "Comparative study on the performance of many-objective and single-objective optimisation algorithms in tuning load frequency controllers of multi-area power systems," *IET Gener. Transmiss. Distrib.*, vol. 10, no. 12, pp. 2915–2923, Sep. 2016, doi: 10.1049/IET-GTD.2015.1334.
[38] H. Abubakr, T. H. Mohamed, M. M. Hussein, and G. Shabib, "ESO-based self tuning frequency control design for isolated microgrid system," in *Proc. 21st Int. Middle East Power Syst. Conf. (MEPCON)*, Dec. 2019, pp. 589–593, doi: 10.1109/MEPCON47431.2019.9008042.
[39] H. Abubakr, J. C. Vasquez, K. Mahmoud, M. M. F. Darwish, and J. M. Guerrero, "Robust PID-PSS design for stability improvment of grid-tied HydroTurbine generator," in *Proc. 22nd Int. Middle East Power Syst. Conf. (MEPCON)*, Dec. 2021, pp. 607–612, doi: 10.1109/MEPCON50283.2021.9686204.
[40] G. Dhiman, K. K. Singh, M. Soni, A. Nagar, M. Dehghani, A. Slowik, A. Kaur, A. Sharma, E. H. Houssein, and K. Cengiz, "MOSOA: A new multi-objective seagull optimization algorithm," *Expert Syst. Appl.*, vol. 167, Apr. 2021, Art. no. 114150, doi: 10.1016/J.ESWA.2020.114150.
[41] S. M. Nosratabadi, M. Bornapour, and M. A. Gharaei, "Grasshopper optimization algorithm for optimal load frequency control considering predictive functional modified PID controller in restructured multi-resource multi-area power system with redox flow battery units," *Control Eng. Pract.*, vol. 89, pp. 204–227, Aug. 2019, doi: 10.1016/J.CONENGPRAC.2019.06.002.
[42] M. Gheisarnejad and M. H. Khooban, "Secondary load frequency control for multi-microgrids: HiL real-time simulation," *Soft Comput.*, vol. 23, no. 14, pp. 5785–5798, May 2018, doi: 10.1007/S00500-018-3243-5.
[43] R. V. Rao, "Jaya: A simple and new optimization algorithm for solving constrained and unconstrained optimization problems," *Int. J. Ind. Eng. Comput.*, vol. 7, no. 1, pp. 19–34, 2016.
[44] J. Derrac, S. García, D. Molina, and F. Herrera, "A practical tutorial on the use of nonparametric statistical tests as a methodology for comparing evolutionary and swarm intelligence algorithms," *Swarm Evol. Comput.*, vol. 1, no. 1, pp. 3–18, Mar. 2011, doi: 10.1016/J.SWEVO.2011.02.002.
[45] H. Bevrani, T. Ise, and Y. Miura, "Virtual synchronous generators: A survey and new perspectives," *Int. J. Electr. Power Energy Syst.*, vol. 54, pp. 244–254, Jan. 2014, doi: 10.1016/J.IJEPES.2013.07.009.
[46] H. Bevrani, B. Francois, and T. Ise, *Microgrid Dynamics and Control*. New York, NY, USA: Wiley, 2017.
[47] S. Manabe, "Importance of coefficient diagram in polynomial method," in *Proc. 42nd IEEE Int. Conf. Decis. Control*, vol. 4, Dec. 2003, pp. 3489–3494.

HUSSEIN ABUBAKR (Graduate Student Member, IEEE) was born in Egypt. He received the Diploma degree in metals from the Industrial Technical Institute for Aluminum, in 2009, and the B.Sc. and M.Sc. degrees in electrical power engineering from Aswan University, Egypt, in 2014 and 2019, respectively. He is currently pursuing the Ph.D. degree with the Center for Research on Microgrids (CROM), Department of Energy Technology, Aalborg University, Denmark.

From 2014 to 2016, he was a Quality Control, Research and Development Engineer with Electronic Construction Services (ECS) Petroleum Company, Cairo, Egypt. From 2019 to 2021, he is working as an Assistant Lecturer with the Faculty of Energy Engineering, Aswan University. Since 2021, he has been an Egyptian Government Scholarship-Holder. His research interests include electrical power system control, optimization techniques implementation and coding, adaptive control, and flexible loads integration, such as electric vehicles EVs, ocean thermal energy conversion (OTEC) systems, renewable energy sources RESs, and microgrids clusters.

JOSEP M. GUERRERO (Fellow, IEEE) received the B.S. degree in telecommunications engineering, the M.S. degree in electronics engineering, and the Ph.D. degree in power electronics from the Technical University of Catalonia, Barcelona, in 1997, 2000, and 2003, respectively.

Since 2011, he has been a Full Professor with the Department of Energy Technology, Aalborg University, Denmark, where he is responsible for the Microgrid Research Program (www.microgrids.et.aau.dk). He has published more than 500 journal articles in the fields of microgrids and renewable energy systems, which are cited more than 30,000 times. His research interests are oriented to different microgrid aspects, including power electronics, distributed energy-storage systems, hierarchical and cooperative control, energy management systems, smart metering, and the Internet of Things for AC/DC microgrid clusters and islanded minigrids; recently specially focused on maritime microgrids for electrical ships, vessels, ferries, and seaports. In 2015, he was elevated as an IEEE Fellow for his contributions on distributed power systems and microgrids. He received the Best Paper Award of the IEEE TRANSACTIONS ON ENERGY CONVERSION, from 2014 to 2015; and the Best Paper Prize of IEEE-PES, in 2015. He also received the Best Paper Award of the *Journal of Power Electronics*, in 2016. During five consecutive years, from 2014 to 2018, he was awarded by Clarivate Analytics (former Thomson Reuters) as a Highly Cited Researcher. He is an Associate Editor for a number of IEEE TRANSACTIONS.

JUAN C. VASQUEZ (Senior Member, IEEE) received the Ph.D. degree in automatic control, robotics, and computer vision from Barcelona Tech—UPC, Spain, in 2009. In 2019, he became a Full Professor with the Department of Energy Technology, Aalborg University, Denmark, where he is currently the Vice Director of the Center for Research on Microgrids (see crom.et.aau.dk). He was a Visiting Scholar with the Center of Power Electronics Systems (CPES), Virginia Tech; and a Visiting Professor with Ritsumeikan University, Japan. He has published more than 500 journal articles in the field of microgrids, which are cited more than 25,000 times. His current research interests include operation, advanced hierarchical and cooperative control, optimization, and energy management applied to distributed generation in AC/DC microgrids, maritime microgrids, advanced metering infrastructures, and the integration of the Internet of Things and energy internet into the smartgrid. Since 2017, he has been awarded by the Thomson Reuters as a Highly Cited Researcher. He was a recipient of the Young Investigator Award, in 2019. He is an Associate Editor of *IET Power Electronics* and the IEEE SYSTEM JOURNAL and a Guest Editor of a Special Issue on the IEEE TRANSACTIONS ON INDUSTRIAL INFORMATICS on "Energy Internet."

TAREK HASSAN MOHAMED was born in 1975. He received the B.Sc. degree in control engineering from Minoufta University, Egypt, and the M.Sc. and Ph.D. degrees in electrical engineering from Minia University, Egypt, in 2006 and 2012, respectively.

From 2006 to 2012, he was an Assistant Lecturer with the Faculty of Energy Engineering, Aswan University. Since 2017, he has been an Assistant Professor with the Electrical Engineering Department, Faculty of Energy Engineering, Aswan University, Egypt, where he has been the Head of the Department, since 2018. He is the author of more than 40 articles. His research interests include automatic control, power system control, and renewable energy.

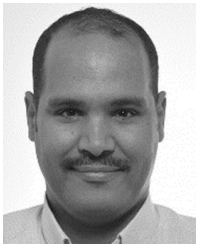

KARAR MAHMOUD (Senior Member, IEEE) received the B.Sc. and M.Sc. degrees in electrical engineering from Aswan University, Aswan, Egypt, in 2008 and 2012, respectively, and the Ph.D. degree from the Electric Power and Energy System Laboratory (EPESL), Graduate School of Engineering, Hiroshima University, Hiroshima, Japan, in 2016. Since 2010, he has been with Aswan University, where he is currently an Associate Professor with the Department of Electrical Engineering, Faculty of Engineering. He has authored or coauthored several publications in top-ranked journals, including IEEE journals, international conferences, and book chapters. His research interests include power systems, renewable energies, smart grids, distributed generation, optimization, applied machine learning, and electric vehicle. Since 2021, he has been a Topic Editor in *Sensors* journal (MDPI) and *Energies* journal (MDPI) and also becomes a Guest Editor for two special issues in *Catalysts* journal (MDPI) and *Forecasting* journal (MDPI).

MOHAMED M. F. DARWISH (Member, IEEE) was born in Cairo, Egypt, in 1989. He received the B.Sc., M.Sc., and Ph.D. degrees in electrical engineering from the Faculty of Engineering at Shoubra, Benha University, Cairo, in May 2011, June 2014, and January 2018, respectively. From 2016 to 2017, he was a Ph.D. Student with the Department of Electrical Engineering and Automation (EEA), Aalto University, Finland, and with the Prof. M. Lehtonen's Group. He is currently working as an Assistant Professor with the Department of Electrical Engineering, Faculty of Engineering at Shoubra, Benha University. He is also a Postdoctoral Researcher with the Department of EEA, School of Electrical Engineering, Aalto University. He has authored in several international IEEE journals and conferences. His research interests include renewable energies, control systems, nano-fluids, fault diagnosis, optimization, applied machine learning, the IoT, Industry 4.0, high voltage, and energy storage systems. He received the Best Ph.D. Thesis Prize that serves the Industrial Life and Society all over the Benha University Staff, for the academic year 2018–2019. Since 2021, he has been a Topic Editor in *Catalysts* (MDPI) journal also becomes a Guest Editor for the special issue in *Catalysts* (MDPI) journal.

YASSER AHMED DAHAB received the B.Sc. and M.Sc. degrees in computer science from Friedrich-Alexander University, Erlangen, Germany, and the Ph.D. degree in information technology from Cairo University, Egypt. His interests include robotics, wireless computer networks, artificial intelligence, and automatic control.